CHARACTERISTICS OF SPENT NUCLEAR FUEL AND CLADDING RELEVANT TO HIGH-LEVEL WASTE SOURCE TERM

Prepared for

Nuclear Regulatory Commission
Contract NRC-02-88-005

Prepared by

Center for Nuclear Waste Regulatory Analyses
San Antonio, Texas

May 1993

CNWRA 93-006

CHARACTERISTICS OF SPENT NUCLEAR FUEL AND CLADDING RELEVANT TO HIGH-LEVEL WASTE SOURCE TERM

Prepared for

Nuclear Regulatory Commission
Contract NRC-02-88-005

Prepared by

Hersh K. Manaktala

Center for Nuclear Waste Regulatory Analyses
San Antonio, Texas

May 1993

PREVIOUS REPORTS IN SERIES

Number	Name	Date Issued
CNWRA 92-017	An Assessment of Borosilicate Glass as a High-Level Waste Form	September 1992
CNWRA 92-018	Leaching of Borosilicate Glass Using Draft ASTM Procedure for High-Level Waste	August 1992

ABSTRACT

This report, based on literature study, describes characteristics of light water reactor (LWR) fuel assemblies for boiling water reactors (BWR) and pressurized water reactors (PWR) and the changes that take place in both cladding and uranium dioxide fuel during service in commercial power reactors. This information is provided as a background for the evaluation of important factors related to fuel stability under geologic repository conditions. Data related to discharged fuel storage (both wet and dry) are also provided, along with the condition of the fuel in terms of damaged and leaking fuel assemblies. The degradation of spent fuel and cladding while in service in the reactor and likely degradation in a geologic repository are discussed in terms of cladding oxidation and corrosion, and fuel-pellet cracking, fuel restructuring, microstructure and fission product mobility, inventory and distribution of fission products, fuel pellet rim effect, and fission gas release and pressure increase. The range of attributes of discharged fuel will have an impact on the releases of radionuclides from the engineered barrier system (EBS) and, as a result, on the compliance with the regulations relating to the gradual release from a repository over a period of 10,000 years. A suggestion has been made to characterize a wider variety of spent LWR fuels, including high burnup fuels and fuels with characteristics outside the range of those currently awaiting geologic disposal, with the intent of including the full range of spent fuel characteristics and performance in developing source term models for performance assessment. A significant portion of this report deals with review of studies on oxidation and release of radionuclides from spent fuels. Although the emphasis is on an oxidizing environment, the likely behavior of spent fuel under a reducing environment has also been discussed. The parameters important for assessment of spent fuel behavior in a geologic repository include oxidation state of the fuel at the time of contact with water, geochemistry of the repository (chemical composition of the leachant), water flow conditions, and synergistic effects due to modification of the geochemical environment as a result of releases from vitrified waste form and corrosion products from the waste package. A number of areas requiring additional experimental data have been identified. Issues related to modeling of source term for use in performance assessments have also been discussed.

CONTENTS

CONTENTS (cont'd)

FIGURES

FIGURES (cont'd)

TABLES

ACKNOWLEDGMENTS

This report was prepared to document work performed by the Center for Nuclear Waste Regulatory Analyses (CNWRA) for the U.S. Nuclear Regulatory Commission (NRC) under Contract No. NRC-02-88-005. The activities reported here were performed on behalf of the NRC Office of Nuclear Material Safety and Safeguards (NMSS), Division of High-Level Waste Management (DHLWM). The report is an independent product of the CNWRA and does not necessarily reflect the views or regulatory position of the NRC.

1 INTRODUCTION

The current Code of Federal Regulations, Title 10 Part 60 Section 113, requires the engineered barrier system (EBS) to provide containment for the high-level radioactive wastes (HLW) for a minimum period of 300 to 1,000 years after permanent disposal in a geologic repository (U.S. NRC, 1990). The regulations also specify performance requirements for the EBS following permanent closure of the repository. The maximum allowable release rates of significant radionuclides from the EBS, following the containment period, is specified as 1 part in 100,000 per year of the inventory of a particular radionuclide calculated to be present at 1,000 years following permanent closure of the repository. According to the regulations, the performance of the repository and engineered barriers are to be calculated for a 10,000-year period. However, it should be noted that this is not intended to be the design life of the repository. Quantitative estimates of near-field releases are also needed to evaluate the far-field migration of radionuclides from the EBS. Such estimates of long-term releases require understanding of property changes of the fuel and modeling of their consequences.

As a step towards developing a better understanding of the important characteristics of the light water reactor (LWR) fuels and cladding that would control the release of radionuclides from the spent fuel in a repository, this report, based on literature, provides an overview of the literature in the field. A number of original figures and tables have been slightly modified or changed. They are shown as 'adapted' from the original reference. All tables and figures used from the literature have been credited to the literature citations. The properties/materials characteristics discussed include composition and radionuclide inventory, fuel-pellet cracking and restructuring, fission gas quantity and composition, helium generation from actinide decay, and likely changes in the oxidation state of the failed/defected spent fuel rods and upon breach of the fuel cladding intact at the time of emplacement.

The report also describes and discusses the experimental data reported in the literature on release of radionuclides from unirradiated and spent fuel when exposed to water vapors and aqueous environments. Processes which may have significant impact on the release of radioactivity from the spent fuel in an unsaturated geologic repository, and which have not been currently addressed in source-term models, have been identified. Incorporation of the suggested processes in the source-term models can be expected to provide more accurate estimates of releases of radionuclides under repository-representative conditions. The processes identified in the report include: (i) spent fuel and cladding degradation during an extended period of high-temperature exposure prior to water intrusion, (ii) extended exposure to high-moisture content atmosphere/small amount of water prior to interaction with groundwaters, (iii) release kinetics of spent fuel with a higher oxidation state than UO_2 discharged from the reactor/storage, (iv) accounting for the estimated 4,000 to 5,000 failed fuel rods (at the time of the beginning of repository operation) in the source term, (v) modification of groundwater chemistry due to radiolysis of repository air/moisture, corrosion products released as a result of waste package degradation/failure, and leached species from vitrified wasteform, (vi) additional releases of ^{14}C from the cladding and spent fuel due to oxidation in the repository prior to contacting groundwaters, (vii) fuel cladding failure as a function of time (which may be a more conservative approach than the so-called 'no-credit' for cladding approach used by the current models), (viii) precipitate and colloid formation phenomena, (ix) microbial activity in the release of radionuclides from spent fuel, and (x) acceleration in the cladding/spent-fuel degradation as a result of galvanic interaction between the cladding, spent fuel, and waste package component materials.

2 CLADDING, FUEL, AND FUEL ASSEMBLY CHARACTERISTICS (AS-FABRICATED)

2.1 FUEL CLADDING MATERIAL

Early nuclear power reactors used stainless steel as a fuel cladding material. The search for an alternative material with improved performance and lower neutron absorption led to the change from stainless steel to zirconium-based alloys. Only 5 out of approximately 114 power reactors in the United States (U.S.) used stainless steel cladding (U.S. DOE, 1992b). The two commonly used cladding materials for fuels are Zircaloy-2 and Zircaloy-4. Both are dilute alloys with more than 97 weight percent zirconium. Their major alloying elements are tin, iron, chromium, oxygen, and silicon, with Zircaloy-2 also containing nickel. Fuel cladding for pressurized water reactors (PWR) is primarily fabricated from Zircaloy-4, while Zircaloy-2 is the material for boiling water reactor (BWR) application. Nickel was removed in Zircaloy-4 to reduce hydrogen pick-up during reactor operation.

2.2 FUEL ROD AND ASSEMBLY DESIGN

Typical LWR fuel consists of stacks of sintered UO_2 pellets in a Zircaloy cladding. The cladding is a long cylindrical seamless tube with approximate dimensions of 4 m length, 9 to 13 mm internal diameter, and 0.5 to 0.8 mm wall thickness. The dimensions depend upon the fuel design. The sealed fuel rods contain UO_2 fuel enriched in ^{235}U in the form of pellets which are approximately 1 cm in length and slightly smaller in diameter than the fuel cladding internal diameter. A plenum, with a coil spring, is provided at the top of the fuel pellet stack for fission gases (Kr, Xe, I_2). The rods are arranged in a square array to form a fuel assembly. The number of rods in each assembly can vary from 49 to 289 in a 7×7 to 17×17 configuration, depending upon the reactor type and the fuel assembly design. There are at least 88 different LWR fuel assembly types which are or have been used in the U.S. (U.S. DOE, 1992b), and additional ones are evolving (Gilbert et al., 1990). Typical BWR and PWR fuel assemblies are shown in Figure 2-1. The BWR fuel assembly typically has a width of 14 cm, a length of 448 cm, and a U content of 183 to 195 kg, while the PWR assembly has a width of 47 cm, a length of 406 cm, and a U content of 425 to 460 kg (U.S. DOE, 1992b). The enrichment of UO_2 in the fissile isotope of uranium, ^{235}U, is approximately 3 percent prior to irradiation, and the fuel-pellets have a sintered density of 94 to 95 percent of the theoretical density. Grain size is uniform and is typically 2 to 4 μm. Fuel rods are pressurized with He to improve heat conduction across the fuel-cladding gap, which also tends to reduce fission-gas release. Additional details of the design features of the existing spent fuel inventory are published in the literature (Moore et al., 1990; Moore and Notz, 1991).

The fuel is typically irradiated at an average linear power of 15 to 25 $kW \cdot m^{-1}$ with a fuel pellet centerline temperature in the range of 800°C to 1200°C. Only a small percentage of the fuel (< 10 percent) in the reactor core has a centerline temperature exceeding 1200°C (Woodley, 1983). Fuel pellet centerline temperature above this limit has a considerable effect on the fission-gas release and microstructural characteristics of the spent fuel. The other major irradiation parameter affecting spent fuel characteristics is the burnup, which is expressed in units of megawatt days per kilogram of uranium ($MWd \cdot kgU^{-1}$). Burnups for fuels have typically ranged from 4 to 35 $MWd \cdot kgU^{-1}$ over the past three decades. Data related to the average burnup and highest burnup, separately for BWR and PWR fuel assemblies discharged during the years 1968 through 1988, are provided in Figure 2-2. The trend clearly indicates increasing burnup for both types of assemblies. Presently, PWR fuels are being developed for burnup of 60 $MWd \cdot kgU^{-1}$ and higher.

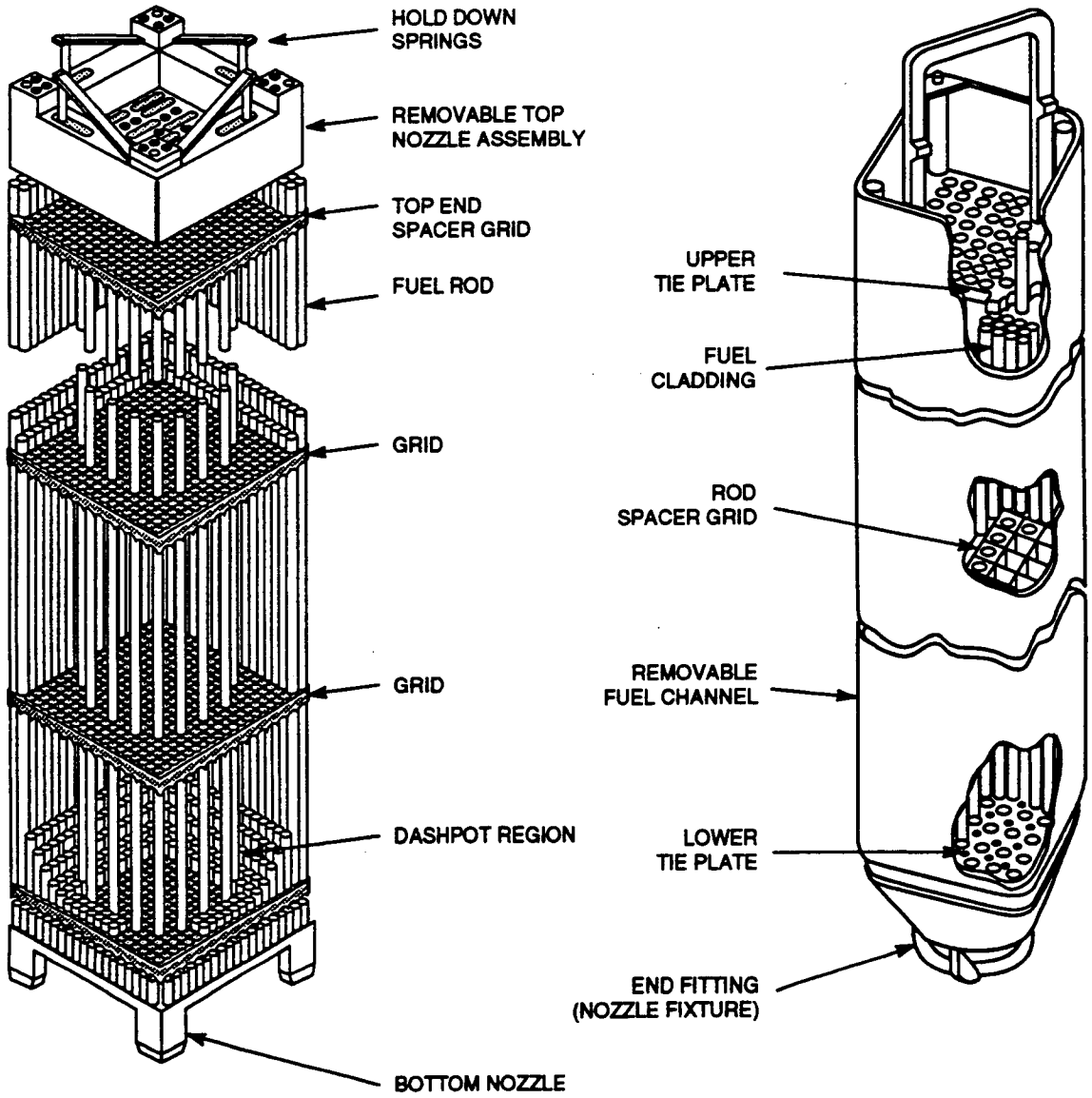

Figure 2-1. Schematic of fuel assembly (a) PWR fuel; (b) BWR fuel

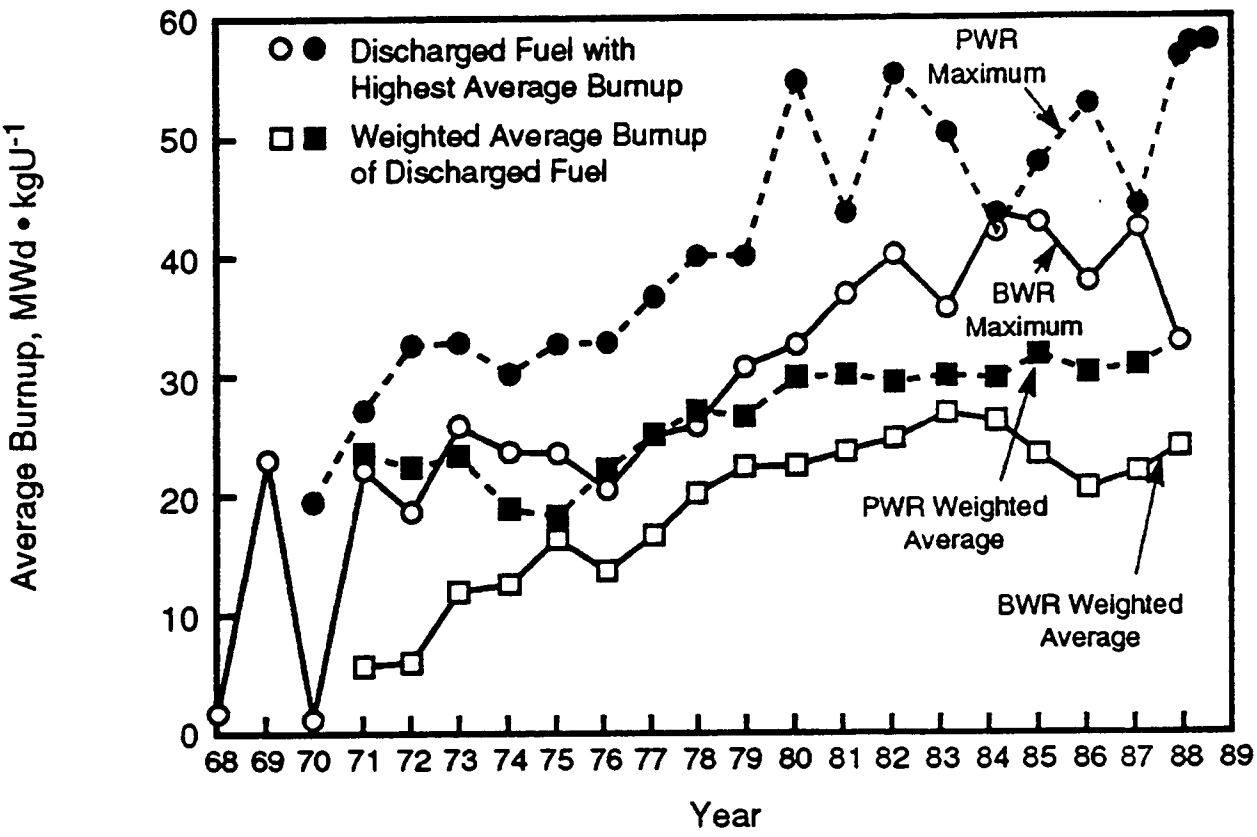

Figure 2-2. Highest and average burnup of LWR spent fuel assemblies currently in storage (Bailey and Johnson, 1990)

The UO_2 fuels have demonstrated satisfactory dimensional and radiation stability as well as chemical compatibility with the cladding and coolant under both BWR and PWR operating conditions. However, a number of changes take place in the physical, structural, and chemical characteristics of the cladding and fuel that could influence radionuclide release under repository environments. These are discussed briefly in this report.

3 REACTOR SERVICE INDUCED CHANGES

3.1 DEGRADATION OF CLADDING IN THE REACTOR

The majority of the past failures of Zircaloy fuel cladding have been attributed to the following seven modes:

- accelerated waterside corrosion
- internal hydriding
- pellet-clad-interaction (PCI)
- fretting and wear
- fuel rod and assembly bow
- neutron irradiation induced growth
- fuel rod collapse or flattening.

Detailed discussion of the above-listed failure modes has been reported in the literature (Garzarolli, 1979). The first three modes, which degrade the cladding in the reactor (whether the fuel rod fails or not), are also considered potential degradation modes that are pertinent to geological disposal of spent fuel. The last four degradation modes are primarily applicable to service in the reactor, and are not likely to be operative in a repository environment. However, there are two additional potential degradation modes of interest for the geological disposal of spent fuel; namely, mechanical stress overloading and stress/creep rupture (Manaktala, 1990; 1991).

3.2 DESIGN MODIFICATIONS

The LWR fuel cladding, fuel rods, and assembly design have evolved over the past two to three decades, resulting in much improvement in the performance—as expressed by the reduction of cladding failures in core (Baily et al., 1979). Significant changes that led to the improvement are summarized in the following sections.

3.2.1 Boiling Water Reactor Fuels

Fuel rod failures due to Zircaloy hydriding, first observed in BWRs in the early 1970s, have been practically eliminated by reducing the amount of moisture introduced during fabrication and by the inclusion of a 'hydrogen getter' within the rod. Moisture was reduced mainly by elevated temperature vacuum drying of the loaded fuel rods. A negligible number, <0.002 percent, of waterside corrosion failures was observed in some early cores in BWRs. These failures were attributed to a drastic increase in the coolant pressure drop, due to heavy deposition of copper-rich 'crud' at the fuel assembly inlet nozzles, leading to the blockage of heat flow by corrosion layers or crud deposits. The source of the crud products was traced to the use of Cu-Ni alloy as tubing material in feedwater heaters. The problem was eliminated by replacing them with stainless steel fabricated units and by effective demineralization and optimization of the oxygen content of the core coolant. The failure due to PCI, initially observed in 1971, has been reduced by: (i) change of reactor operating procedures to avoid sharp ramps in power levels, especially after mid-life of the fuel in core, (ii) introduction of fuel rods with smaller diameters, resulting in reduced linear heat output of the rod, (iii) fuel-design improvements, for example, short chamfered pellets and annealed cladding, (iv) addition of plasticizer in the fuel pellets, for example, alumino-silicates to reduce the stress level on the cladding upon localized pellet-clad interaction, and

(v) use of a low-oxygen unalloyed zirconium liner bonded to the cladding inner surface—that is, a ductile barrier between the fuel and the Zircaloy cladding. Another design change, implemented in 1977, was the increase in helium internal pressure of the fuel rod from 1 to 3 atm. This resulted in reducing the fuel operating temperatures. At lower fuel temperatures, fission gas and the more volatile fission products have lower mobility for migration into the fuel-cladding gap through grain boundaries and pellet cracks. Reduced migration led to reduced potential for environment embrittlement of the cladding and fewer stress corrosion related failures. It is generally agreed that I_2 and probably Cs/Cd are the predominant embrittling agents.

3.2.2 Pressurized Water Reactor Fuels

The evolutionary changes in PWR fuel design include the use of greater fuel rod pressurization than in BWR fuel rods to prevent cladding collapse onto the fuel due to the higher system pressure (fuel rod internal pressure was increased from 1 to about 30 atm of helium) (Andrews et al., 1979). Also, the UO_2 fuel pellet fabrication parameters were modified to yield pore size density and distribution which made the fuel less prone to radiation-induced sintering in the reactor. Densification of fuel pellets in service has been known to cause fuel column shortening, formation of gaps in the fuel column, and increase in the gap between the fuel and cladding. This phenomenon has led to cladding collapse in PWRs and, in some cases, to the release of fission products in the coolant. Although fuel rod failures due to PCI have been fewer in PWRs than in BWRs, some of the remedies implemented for BWRs have been introduced in PWR fuel rods or are being considered. These include shorter and chamfered fuel pellets, revised operating guidelines for core power increases (less severe ramp-ups), and use of a zirconium liner.

The frequency of cladding failures has been reduced progressively over the past few decades from 2 percent or more in some BWR cores to 0.01 to 0.02 percent in both BWRs and PWRs, at present. According to industry estimates, this low failure level is expected to be maintained (Locke, 1975; Garzarolli et al., 1979). The frequencies of failures due to various modes reported in the literature are illustrated in Figure 3-1. The progressively reducing trends are evident from Figure 3-2. The dramatic improvement in the fuel rod failures, to a large extent, is a result of a series of design modifications, the salient ones described earlier. Neither technical nor economical justification is suggested for reducing the fuel failure level below 0.01 percent (Locke, 1975). Consequently, in the inventory of spent fuel, one can anticipate at least 1 in every 10,000 rods to be breached. The spent fuel rods with breached cladding obviously pose a much greater risk for release of fission products to the geological repository. Therefore, additional contribution to the near-field source term needs to be incorporated in performance assessment models/codes to account for breached cladding. The models should also account for rods that may be breached in handling during waste package loading, assembling, and transportation to the repository for emplacement.

3.3 DEGRADATION OF FUEL IN THE REACTOR

After irradiation in a nuclear reactor, the composition of the fuel becomes more complex. Along with the original uranium dioxide, the spent fuel pellets contain gaseous and solid fission products. These are generally distributed inhomogeneously. Additional variability in the characteristics of the spent fuel results from reactor operating power levels, location of the fuel in core, and total burnup of the fuel assembly. Some of the significant changes are described as follows.

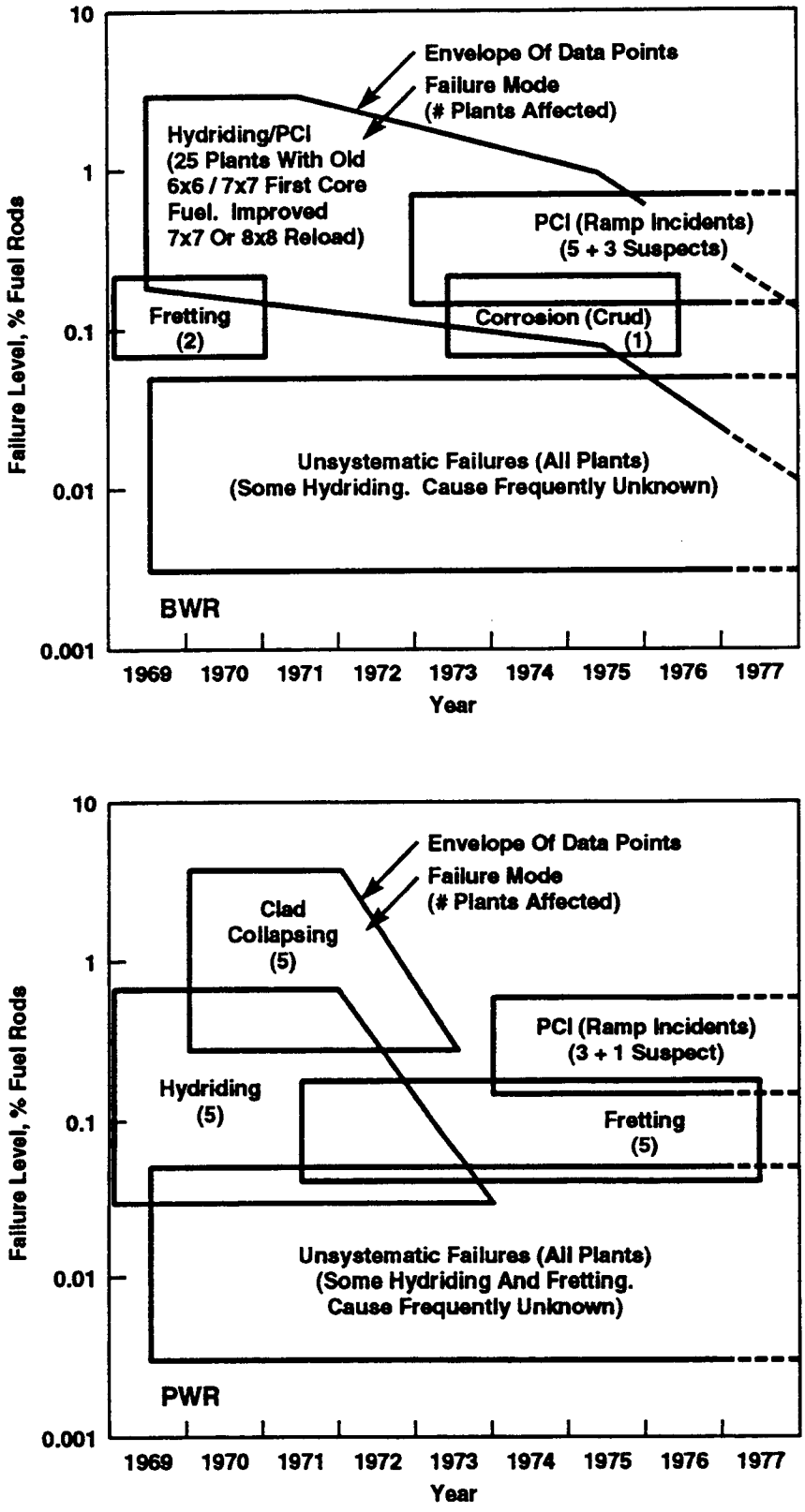

Figure 3-1. Fuel rod failures in LWRs for the years 1969-1977 (Garzarolli and Stehle, 1979)

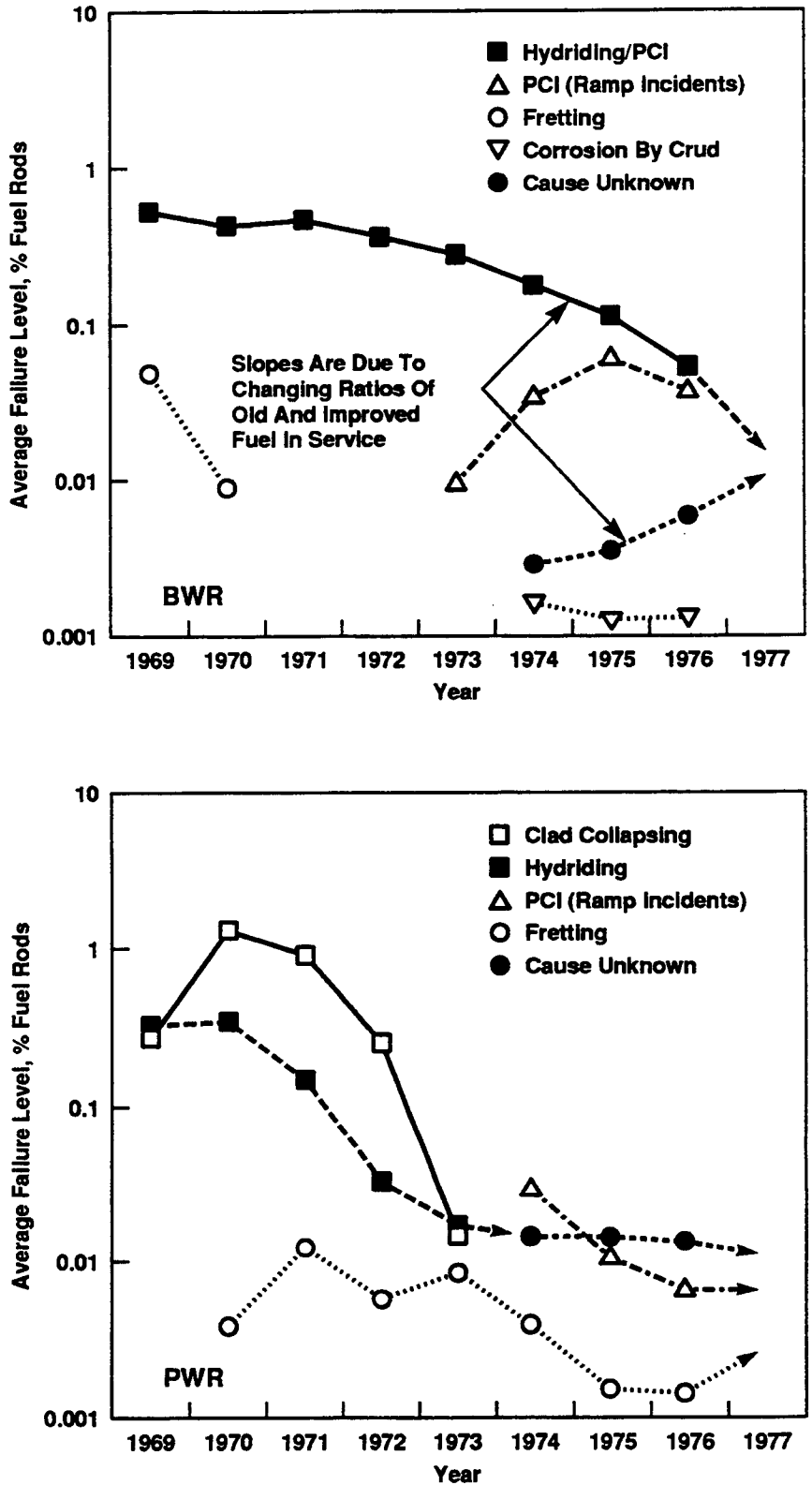

Figure 3-2. Fuel rod failure trends in LWRs for the years 1969-1977 (Garzarolli and Stehle, 1979)

3.3.1 Fuel-Pellet Cracking

During operation in a reactor, the steep thermal gradient in the fuel and the fracture strength of UO_2 leads to cracking of the pellets. The resulting cracks provide pathways for radial migration of volatile fission products to the pellet-cladding gap, and also increase the surface area of the fuel that could be exposed to vapor/gas and groundwater in a repository. No systematic study of the surface area increase of the fuel as a result of pellet cracking is available. However, post-irradiation examination (PIE) on a limited number of fuel pellets indicates an increase in the crack density in the high-power fuels. Particle sizes reported for irradiated PWR fuel with an average burnup of 28 $MWd \cdot kgU^{-1}$ range from 2 to 6.73 mm for 86 weight percent of the fuel, with less than 0.08 weight percent smaller than 0.1 mm in diameter (Katayama et al., 1980). In the same study, it has been reported that the surface area of the fuel increased from an estimated 38 $mm^2 \cdot mm^{-1}$ of fuel length to more than 100 $mm^2 \cdot mm^{-1}$ of fuel length as a result of irradiation. Since the surface area and the size distribution of the fuel particles are likely to be factors that would control the release rate of radionuclides from the fuel upon contact with water, such data may need to be considered in developing source-term models.

3.3.2 Fuel Restructuring

Fuel restructuring involves physical and chemical changes, including grain growth, central void formation, fission gas bubble formation and release, formation of metallic ingots, and migration of volatile compounds within and outside the fuel pellets, depending on their vapor pressures. As stated earlier, LWR fuel rods typically operate at 15 to 25 $kW \cdot m^{-1}$. At these linear powers, the fuel centerline temperature is less than 1200°C for a typical fuel (Guenther and Barner, 1981). A review of literature on fuel rod performance indicates that equiaxed grain growth (restructuring) requires temperatures in the range of 1300°C to 1650°C, depending upon the fuel type and fuel rod design (Olander, 1976). Therefore, at typical operating linear power, little if any restructuring of the fuel pellets would be expected. This has been confirmed by a reported examination of PWR spent fuel with an average burnup of 28 $MWd \cdot kgU^{-1}$ (Katayama et al., 1980). However, a small portion of a typical reactor core is likely to be operated at a high enough fuel centerline temperature to result in the restructuring of a small fraction of the core load. The current trends point toward higher burnup and a higher operating temperature. These trends may require that consequences of restructured spent fuels be considered in developing source-term models.

3.3.3 Microstructure and Fission-Product Mobility

At low temperatures (i.e., below centerline temperatures of 1000°C), fission products are expected to remain in the vicinity of the fission recoil position, since their diffusion coefficients in UO_2 are typically $< 10^{-21}$ $m^2 \cdot s^{-1}$ (Johnson and Shoesmith, 1988). Therefore, limited, if any, microstructural changes are likely to occur in the majority of the fuel. Unfortunately, little data from direct observations are available regarding the size, composition, and location of fission-product phases in UO_2 fuel irradiated at fuel centerline temperatures less than 1200°C. This is due, perhaps, to the difficulty in experimentally detecting submicroscopic phase segregations. Since a substantial portion of the reactor core operates in the 1000°C to 1200°C fuel centerline temperature range, additional investigations of LWR fuels operating in this temperature range may be desirable.

When fuel centerline temperatures exceed the 1200°C to 1300°C range, fission-product phase segregation begins to become significant. At these temperatures, the diffusion coefficients increase sufficiently to permit accumulation of volatile fission products in inter- and intra-granular pores, leading

to fission product accumulations on the grain boundaries and an increase in the fuel grain size. The intersection of cracks in the fuel pellets with intergranular porosity reportedly results in the release of volatile species, such as Xe, Kr, Cs, and I, to the void spaces in the fuel rod. At even higher fuel centerline temperatures of 1800°C and above, noble metal inclusions up to 10 μm in diameter have been observed, and, in one study, up to 50 percent of Mo in the fuel was found in metallic inclusions (Kleykamp, 1979). The remainder was believed to be distributed submicroscopically throughout the fuel. Yet another study reported the detection of small ingots (about 1 μm or smaller in diameter) of noble metal at the center of a PWR spent fuel (Barner, 1984). In general, metallic fission products, such as Mo and Ru, and, to a lesser extent, Tc, Pd, and Rh, develop in fuel irradiated to high burnup (Yang and Olander, 1981; Adachi et al., 1988). Although such high fuel operating temperatures are outside the normal operating range for the majority of the fuel in current design LWR cores, a small part of the discharged fuel could show substantial segregation of noble metal phases. A significant presence of noble metal phases and their distribution and morphology could alter the radionuclide release rates from the spent fuel as such phases have very low solubility in aqueous solutions (Pearcy and Manaktala, 1992).

3.3.4 Inventory and Distribution of Fission Products

Of the 103 known elements, 81 are found in spent LWR fuels; of these, 57 have radioactive isotopes in spent fuel. Only limited data are reported in the literature on actual distribution of the fission and reaction products within the fuel grains, at the grain boundaries, or in the fuel-cladding gap. In one of the few experimental studies on this subject reported in the literature, data and estimates are provided for selected radionuclides as shown in Table 3-1.

The results from another study, providing the calculated total fission product and actinide inventories for LWR fuel with a typical burnup of 33 $MWd \cdot kgU^{-1}$, are shown in Table 3-2. The data reported are for radionuclide inventory, taking into consideration decay times ranging from 0 (time of discharge from the reactor) to 10,000 years. It should be noted that a wide variation could be expected in the isotopic composition of the various radionuclides, depending upon the initial composition and enrichment, burnup, reactor operating conditions, type of reactor, and other fuel and service conditions. The calculated results of sensitivity analyses on 10-year old fuels are shown in Table 3-3. The values are given for a number of typical fuel enrichments for both BWR and PWR fuels (Gray et al., 1992).

In an experimental investigation of the reaction of fission products at the fuel cladding inner surface, it has been reported that Ce (and to a lesser extent, Rb) can move by vapor transport to cooler parts of the fuel rod, such as the cladding inner surface or the plenum region. Other fission products that can vaporize and are believed to migrate to the cladding are reported to be: Cs (Rb) in compounds; I (Br) and Te (Se) in compounds with Cs; elemental Ce, Sb, Ag, Sn, and Pb; Ba, as BaO; and possibly MoO_2 (Cubicciotti et al., 1976). Limited information is currently available on the quantities of these elements and compounds in the fuel and/or at the cladding surface, making it difficult to incorporate their releases into the source-term computational models.

3.3.5 Fuel Pellet Rim Effect

The structure and fission product inventory within a few μm of the fuel pellet edge (the 'rim') are affected by neutron flux that peaks at the pellet edge in LWR fuels. This results in higher concentrations of fission products near the fuel edge than at the fuel center (Guenther et al., 1990). Porosity increases in the fuel at the pellet edge as burnup increases. This phenomenon has been attributed

Table 3-1. Fractional distribution of radionuclides in LWR spent fuel (Wuertz and Ellinger, 1985)

Nuclides Analyzed	Nuclides of Similar Chemical Characteristics	Fractional Distributions		
		Fuel-cladding Gap	Grain Boundaries	Fuel Matrix
^{137}Cs	^{87}Rb ^{135}Cs	0.05 0.05	0 0	0.95 0.95
^{155}Eu	^{147}Sm ^{151}Sm	0.01 0.01	0 0	0.99 0.99
^{106}Ru	^{93}Zr ^{99}Tc ^{107}Pd ^{94}Nb	0.03 0.015 0.015 0.9	0.2 0.485 0.485 0	0.77 0.5 0.5 0.1
^{129}I	^{79}Se	0.015	0	0.985
^{125}Sb	^{126}Sn	0.015	0.485	0.5
U	U-Isotopes	0.008	0	0.992
Pu	Pu-Isotopes	0.008	0	0.992
^{241}Am	Am-Isotopes	0.008	0	0.992
^{237}Np	Np-Isotopes	0.008	0	0.992

to enhanced fission gas release that has been observed in high burnup fuels, normally >40 MWd $\cdot$ kgU^{-1} (Einziger and Strain, 1986). A comparison of the porosity ('rim' effect) for fuels of relatively low burnup, 33 MWd $\cdot$ kgU^{-1}, and relatively high burnup, 44 MWd $\cdot$ kgU^{-1}, is shown in Figure 3-3. It is also reported that Cs concentration shows a maximum near the fuel edge in proportion to the burnup in both fuels, although the data has not been reported (Guenther et al., 1990). The α-activity distribution is plotted on an arbitrary scale, normalized to the activity at the pellet center and refers only to the distribution 10 years after discharge from the reactor and approximately halfway through fragment corrosion tests. The phenomenon of fuel structure at the rim with a resultant enhanced release of fission products from high burnup fuel may be important in evaluating results of spent fuel leaching tests. Since the fuel pellets are small in diameter, with relatively large surface-to-volume ratio, the enhanced release of fission products from the rim of high burnup fuels may need to be explicitly incorporated in the source-term models.

Table 3-2. Activity of selected radionuclides in a PWR fuel assembly irradiated to an average burnup of 33 MWd · kgU^{-1}* (adapted from Woodley, 1983)

Radionuclide	Activity (curies)						
	Discharge	1 yr	10 yr	100 yr	300 yr	1000 yr	10,000 yr
^{241}Am	5.015E 01	1.397E 02	7.740E 02	1.731E 03	1.269E 03	4.139E 02	4.734E−03
^{243}Am	7.621E 00	7.631E 00	7.625E 00	7.563E 00	7.427E 00	6.971E 00	3.084E 00
^{14}C	6.853E−01	6.852E−01	6.844E−01	6.770E−01	6.608E−01	6.072E−01	2.044E−01
^{135}Cs	1.711E−01	1.714E−01	1.714E−01	1.714E−01	1.714E−01	1.714E−01	1.709E−01
^{137}Cs	4.786E 04	4.677E 04	3.801E 04	4.785E 03	4.783E 01	4.777E−06	0.0
^{237}Np	1.403E−01	1.436E−01	1.450E−01	1.914E−01	2.883E−01	4.613E−01	5.435E−01
^{238}Pu	9.832E 02	1.054E 03	1.001E 03	4.970E 02	1.052E 02	4.867E−01	6.144E−20
^{239}Pu	1.400E 02	1.424E 02	1.424E 02	1.421E 02	1.413E 02	1.387E 02	1.084E 02
^{240}Pu	2.358E 02	2.358E 02	2.361E 02	2.352E 02	2.305E 02	2.145E 02	8.525E 01
^{242}Pu	8.294E−01	8.295E−01	8.295E−01	8.294E−01	8.291E−01	8.281E−01	8.147E−01
^{226}Ra	5.867E−09	1.104E−08	1.457E−07	1.145E−05	1.142E−04	1.336E−03	5.733E−02
^{90}Sr	3.493E 04	3.408E 04	2.729E 04	2.964E 03	2.138E 01	6.780E−07	0.0
^{99}Tc	6.095E 00	6.124E 00	6.124E 00	6.122E 00	6.118E 00	6.104E 00	5.927E 00
^{126}Sn	3.577E−01	3.577E−01	3.577E−01	3.575E−01	3.570E−01	3.553E−01	3.338E−01

* The fuel assembly initially contained 461 kgU, enriched to 3.2% in ^{235}U.

Table 3-3. Results of sensitivity test cases for 10-year-old fuel (Welch et al., 1990)

Nuclide	Reference PWR Composition, grams	Ratio of Test Case to Reference Case						
		BWR Standard Burnup Cross Sections	Low Enrichment PWR	High Enrichment PWR	Constant Flux PWR	Extended-burnup Cross Section PWR	Constant Actinide Cross Section PWR	Low Power Level
Activation Products								
^{14}C	3.E−01	1.08	1.25	0.81	1.00	0.91	0.97	1.00
^{60}Co	2.E+00	0.34	1.22	0.82	0.99	0.98	0.97	0.97
^{59}Ni	4.E+01	0.25	1.21	0.83	1.00	0.91	0.97	1.00
^{125}Sb	1.E−01	2.35	1.23	0.81	0.98	1.12	0.96	0.94
Fission Products								
^{85}Kr	1.E+01	0.94	0.89	1.08	0.99	0.98	0.99	0.98
^{90}Sr	3.E+02	0.97	0.86	1.10	1.00	0.97	0.99	0.99
^{90}Y	9.E−02	0.97	0.86	1.10	1.00	0.97	0.99	0.99
^{106}Ru	1.E−01	0.75	1.28	0.78	0.94	1.04	1.03	0.90
^{103}Rh	4.E+02	0.96	1.04	0.98	1.00	1.02	1.02	0.99
^{125}Sb	1.E+00	0.84	1.17	0.86	0.98	1.07	0.99	0.95
^{131}Xe	4.E+02	0.96	0.97	1.03	1.00	0.99	1.02	1.00
^{133}Cs	1.E+03	0.99	0.97	1.03	1.00	0.99	1.01	1.00
^{134}Cs	3.E+00	0.94	1.15	0.85	0.97	1.06	0.96	0.96
^{137}Cs	8.E+02	0.98	1.00	1.00	1.00	1.00	1.00	0.99
^{143}Nd	7.E+02	1.00	0.90	1.09	1.00	1.03	1.01	1.00
^{149}Sm	3.E+00	0.87	0.97	1.05	0.91	1.14	1.02	0.88
^{151}Sm	1.E+01	1.06	0.99	1.03	1.00	1.21	1.05	0.98
^{154}Eu	1.E+01	1.03	1.25	0.79	0.99	1.06	0.97	0.99
^{155}Eu	2.E+00	1.05	1.25	0.80	0.99	1.14	0.99	0.99
^{155}Gd	8.E+00	1.13	1.25	0.80	0.99	1.14	0.99	0.99

Table 3-3. Results of sensitivity test cases for 10-year-old fuel (Welch et al., 1990) (cont'd)

Nuclide	Reference PWR Composition, grams	Ratio of Test Case to Reference Case						
		BWR Standard Burnup Cross Sections	Low Enrichment PWR	High Enrichment PWR	Constant Flux PWR	Extended-burnup Cross Section PWR	Constant Actinide Cross Section PWR	Low Power Level
Actinides								
^{230}Th	6.E−03	1.10	0.89	1.09	1.00	0.98	1.02	1.04
^{234}U	1.E+02	1.00	0.90	1.08	1.00	0.99	1.01	1.00
^{235}U	7.E+03	1.03	0.48	1.72	1.00	1.13	1.04	1.00
^{236}U	3.E+03	1.01	0.71	1.22	1.00	0.98	0.99	1.00
^{238}U	9.E+05	1.00	1.00	0.99	1.00	1.00	1.00	1.00
^{237}Np	4.E+02	1.04	0.92	0.97	1.00	1.10	0.97	1.00
^{238}Pu	1.E+02	1.24	1.21	0.76	1.01	1.17	0.99	1.03
^{239}Pu	5.E+03	0.93	1.03	0.96	1.00	1.15	0.86	1.00
^{240}Pu	2.E+03	0.96	1.10	0.88	1.00	1.02	0.66	1.00
^{241}Pu	7.E+02	1.05	1.19	0.79	1.00	1.19	1.24	0.99
^{242}Pu	4.E+02	1.07	1.56	0.61	0.99	1.04	1.25	1.00
^{241}Am	4.E+02	1.09	1.19	0.79	1.00	1.19	1.23	1.01
^{243}Am	7.E+01	1.21	1.96	0.49	0.99	1.14	1.22	1.00
^{242}Cm	3.E−03	1.81	1.22	0.77	1.10	1.31	1.15	1.19
^{244}Cm	1.E+01	1.35	2.58	0.38	0.99	1.24	1.12	1.00
^{246}Cm	7.E−02	1.48	3.94	0.25	0.99	1.28	0.99	1.00

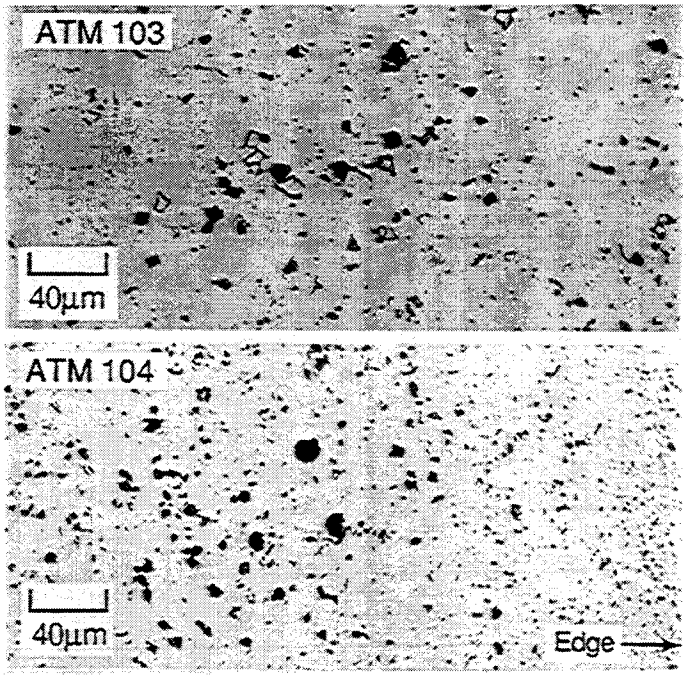

Figure 3-3. Typical porosity near the fuel pellet edge (Burnup: on ATM-103 — 33 MWd · kgU^{-1}; on ATM-104 — 44 MWd · kgU^{-1}) (Guenther et al., 1990)

3.3.6 Fission Gas Release and Pressure

Typical end-of-life (EOL) room temperature pressures for BWR and PWR fuel rods have been reported to be approximately 1.5 MPa and in the 3 to 4 MPa range, respectively (Johnson et al., 1982). Other factors, such as storage temperature and actinide decay, are also likely to affect the gas pressure in an intact fuel rod. Calculated pressure increases, as shown in Figure 3-4, have been reported due to He production from actinide decay over a 10,000-year period (VanLuik et al., 1987; Johnson and Gilbert, 1983). These increases have been calculated for temperatures of 380°C and 100°C, which reportedly represent a conservative peak design temperature (380°C) for the early part of spent fuel life in a geological repository and a typical temperature (100°C) calculated for the end of the containment period. The calculations are based on a PWR fuel rod with 36 MWd · kgU^{-1} burnup and an assumed 100 percent He release.

The isotopic composition of the gas in the plenum, gap, and cracks between the fuel fragments is difficult to estimate accurately because of power history dependence and radioactive decay. However, prepressurization of the fuel rods with He typically leads to a reduction in the fission gas release by as much as an order of magnitude, as shown in Figure 3-5 for pressurized and unpressurized BWR and PWR fuel rods. Most of the gas is composed of Xe, Kr, Ar, and He, with small contributions from other gases such as H_2, CO_2, N_2, O_2, and volatile organic compounds. In an investigation reported in the literature, He constituted about 98 percent, and Xe, Kr, and Ar together accounted for about 1 percent,

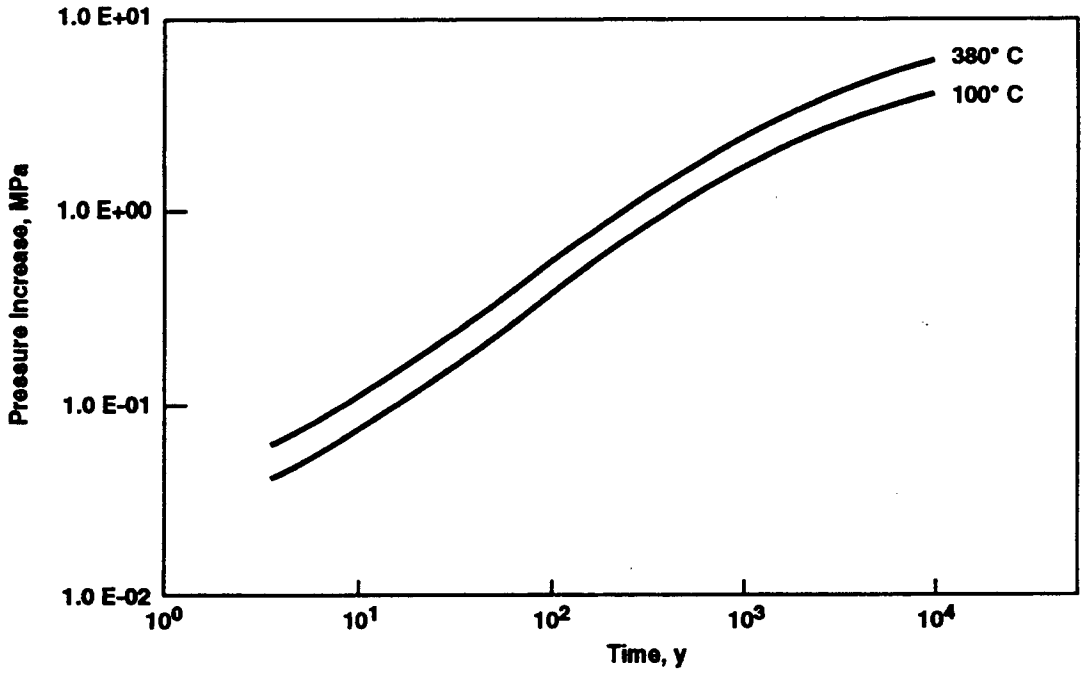

Figure 3-4. Calculated pressure increase caused by helium production from actinide decay (Johnson and Gilbert, 1983)

while all the remaining gases constituted about 1 percent of the total volume (Barner, 1984). Apart from the isotopic changes that result from radioactive decay, the amount of volatile fission products in the free void volume of an intact fuel rod is expected to remain constant after discharge, as long as the fuel temperature remains below 1000°C (Fish and Einziger, 1981). It is further reported that nearly all of the fission gas is retained in the fuel pellets, even after 10 years of spent fuel pool storage, and this would probably be valid for dry storage as well (Fish and Einziger, 1981). Additional fission gas would not be expected to be released under repository storage temperatures unless the fuel cladding ruptures and UO_2 oxidizes to U_3O_8 or higher oxidation states that rearrange and open the lattice structure, creating a much larger fuel surface area from which the gas could be released. Oxidation studies of spent UO_2 fuel have shown that cumulative release of ^{85}Kr and the change in the oxygen-to-metal (uranium) (O/M) ratio track each other in Advanced Gas Reactor (AGR) fuel oxidized above 250°C (Bennett et al., 1987; Williamson and Beetham, 1987). In a study on oxidation of spent AGR fuels, it is reported that even after complete oxidation of UO_2 to U_3O_8, a large fraction of gas remains in the fuel matrix. The amount reported for release of ^{85}Kr is between 7 and 30 percent (Wood et al., 1985). No measurements of release have been made at temperatures likely to dominate the majority of the repository performance calculational times. Although data from comparable tests on LWR fuels (BWR and PWR) as they oxidize from UO_2 to U_3O_8, which could be used for modeling gaseous release due to fuel oxidation, are not available, it is believed that similar trends will hold (Einziger, 1991). Such a scenario for the oxidation of spent LWR fuel is a distinct possibility in an unsaturated repository during the period when the spent fuel temperature is still high (e.g., in the range above 250°C).

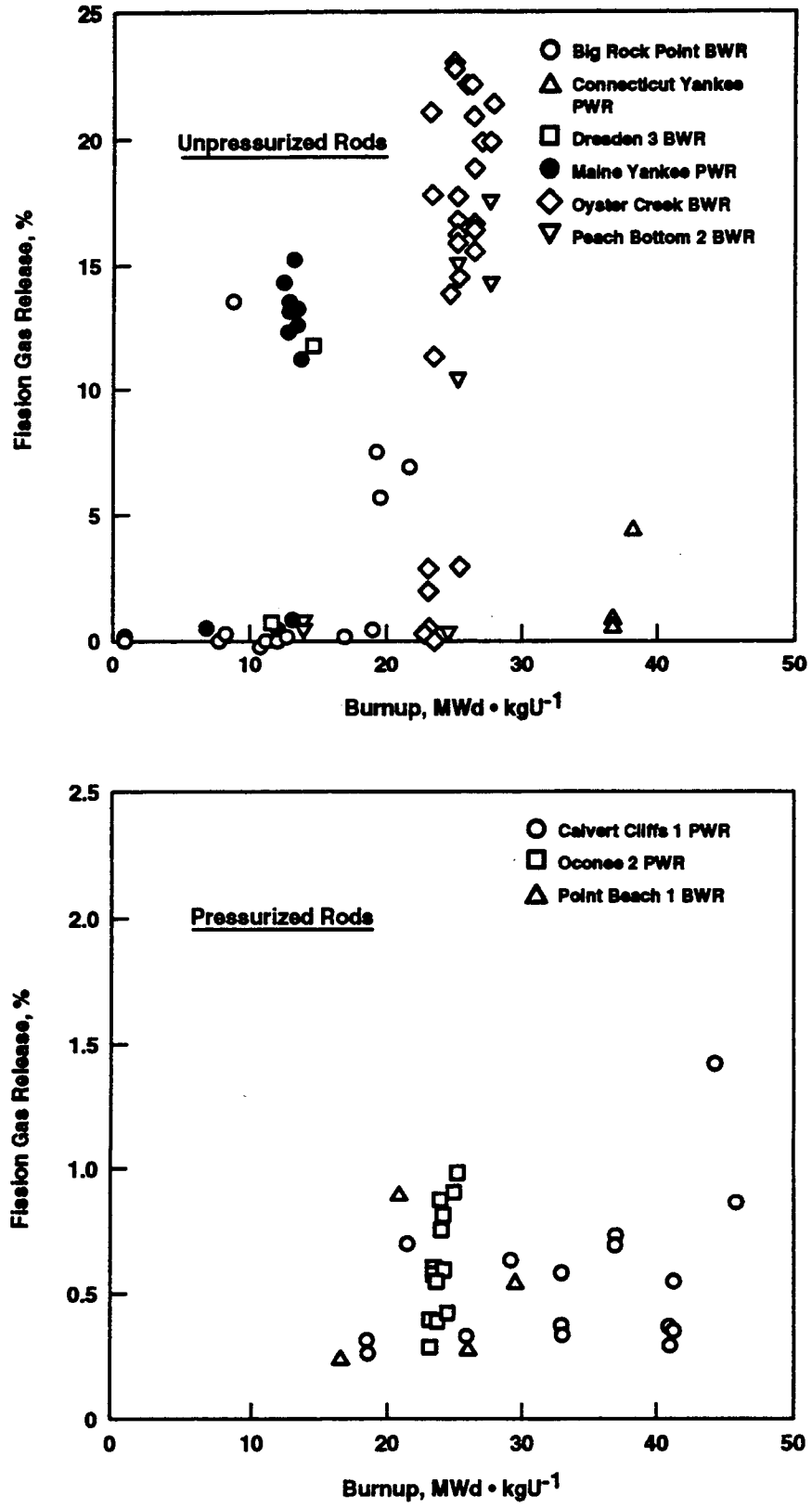

Figure 3-5. Comparison of fission gas release from unpressurized and pressurized LWR fuel rods as a function of the fuel burnup (Ocken, 1982)

4 SPENT FUEL AND CLADDING CHARACTERISTICS, STORAGE, AND INVENTORY

4.1 RADIOACTIVITY ASSOCIATED WITH CLADDING

The radioactivity in spent fuel Zircaloy cladding results mainly from (i) the formation of activation products such as ^{125}Sb and ^{60}Co by neutron irradiation of alloy constituent (Sn) or impurities, (ii) the recoil-implantation of fission products such as ^{137}Cs and ^{106}Ru, and radionuclides, such as ^{134}Cs and ^{154}Eu, produced by neutron capture of recoil-implanted fission products, (iii) the capture of ^{3}H produced in fuel and/or reactor coolant, and (iv) the occlusion of actinides and fission products into the inner surface layer of cladding during irradiation. In addition, activation products (^{60}Co, ^{54}Mn) from piping and structural materials in-core get incorporated in the crud deposited on the fuel rods. The results of a study on Zircaloy-4 cladding of spent PWR fuel with burnup in the 7 to 40 $MWd \cdot kgU^{-1}$ range are summarized in Table 4-1.

4.1.1 Radioactivity as a Function of Fuel Burnup

Figure 4-1 shows the activities of α-emitters on the inner and outer surfaces of cladding as a function of burnup of fuel. The activity of α-emitters on the inner surface of cladding increases with the 3.1 power of fuel burnup, while that on the outer surface increases with the 1.3 power. On the other hand, the gross α-activity of the fuel, as shown in Figure 4-2, increased with the power of 2 of the burnup of fuel. These results indicate a preferential accumulation of α-emitters on the inner surface relative to the outer surface. Figure 4-3 shows the activities of representative β- and γ-emitters in spent nuclear fuel claddings as a function of burnup of fuel. The fission products ^{137}Cs, ^{106}Ru, ^{3}H, and the activation product ^{60}Co in the claddings increase proportionately to the first power with burnup of fuel, whereas the radionuclides ^{134}Cs and ^{154}Eu increase with the power of 2 of the burnup of fuel. These results suggest that, although single events such as fission reaction of ^{235}U produced directly the former radionuclides, the successive reaction with neutrons, that is, the neutron capture after fission reaction, participated in the formation process of the latter radionuclides. As a result, the formation of ^{134}Cs and ^{154}Eu appears to show second-order dependence on the burnup.

4.1.2 Distribution of Radionuclides

The activities of radionuclides in the etching solutions obtained by step-wise etching of the cladding from the inner surface are shown in Table 4-2 and Table 4-3. The data represent cladding from PWR fuel with 29.4 $MWd \cdot kgU^{-1}$ burnup. Table 4-2 shows that more than 98 percent of the fission products, such as ^{137}Cs and ^{106}Ru, are distributed within about 10 μm from the inner surface, while the activation products (^{60}Co, ^{125}Sb) are distributed homogeneously in the interior of the cladding except in the oxide film on the outer surface, where they are relatively enriched. The heterogeneous distribution of ^{3}H was found in the cladding at high burnup, although it was virtually homogeneous in the cladding with low burnup. This implies that segregation of ^{3}H occurs as a hydride in the cladding at high burnup. Since Zircaloy cladding amounts to almost 300 g per kg of UO_2 fuel, and it has a considerable surface area, its leaching properties for the release of radionuclides may be of interest in developing source-term models. Table 4-3 shows that α-emitters are principally present on the inner and outer surfaces, and only a small amount is distributed in the interior of the cladding. The α-emitters concentration ranged from 1.3 to 36 $kBq \cdot g^{-1}$, except for the inner (<3.7 μm in depth) and the outer (>617 μm in depth) surface

Table 4-1. Concentration of radionuclides in the spent fuel claddings (adapted from Hirabayashi et al., 1990)

Burnup (MWd • kgU^{-1})	Concentration of Radionuclides (Bq • g^{-1} cladding)								
	^{3}H	^{54}Mn	^{60}Co	^{106}Ru	^{125}Sb	^{134}Cs	^{137}Cs	^{144}Ce	^{154}Eu
6.9	3.41×10^{6}	5.92×10^{4}	3.52×10^{5}	1.74×10^{6}	1.04×10^{7}	3.04×10^{5}	3.06×10^{6}	9.79×10^{5}	3.26×10^{4}
8.3	—	6.64×10^{4}	4.15×10^{5}	2.11×10^{6}	1.17×10^{7}	4.40×10^{5}	4.58×10^{6}	9.98×10^{5}	4.58×10^{4}
14.6	1.12×10^{7}	1.11×10^{5}	7.48×10^{5}	6.60×10^{6}	2.14×10^{7}	1.74×10^{6}	9.74×10^{6}	1.34×10^{6}	2.22×10^{5}
15.3	1.67×10^{7}	1.16×10^{5}	7.62×10^{5}	5.21×10^{6}	2.23×10^{7}	1.73×10^{6}	9.85×10^{6}	1.85×10^{6}	2.12×10^{5}
21.2	2.24×10^{7}	1.14×10^{5}	9.10×10^{5}	6.19×10^{6}	2.43×10^{7}	3.05×10^{6}	1.37×10^{7}	2.19×10^{6}	4.01×10^{5}
29.4	3.19×10^{7}	1.41×10^{5}	1.30×10^{6}	9.51×10^{6}	3.44×10^{7}	6.53×10^{6}	2.32×10^{7}	—	8.62×10^{5}
32.1	3.40×10^{7}	1.48×10^{5}	1.45×10^{6}	1.10×10^{7}	3.73×10^{7}	7.96×10^{6}	2.59×10^{7}	2.83×10^{6}	1.04×10^{6}
33.6	3.59×10^{7}	1.33×10^{5}	1.42×10^{6}	1.01×10^{7}	3.51×10^{7}	8.13×10^{6}	2.71×10^{7}	3.48×10^{6}	1.03×10^{6}
34.0	3.81×10^{7}	1.53×10^{5}	1.51×10^{6}	1.17×10^{7}	2.78×10^{7}	9.19×10^{6}	2.95×10^{7}	—	1.21×10^{6}
38.1	3.77×10^{7}	—	8.86×10^{5}	1.46×10^{5}	4.37×10^{7}	1.03×10^{7}	3.11×10^{7}	—	1.36×10^{6}
38.7	3.50×10^{7}	8.69×10^{4}	8.08×10^{5}	1.43×10^{7}	4.30×10^{7}	1.06×10^{7}	3.08×10^{7}	—	1.42×10^{6}

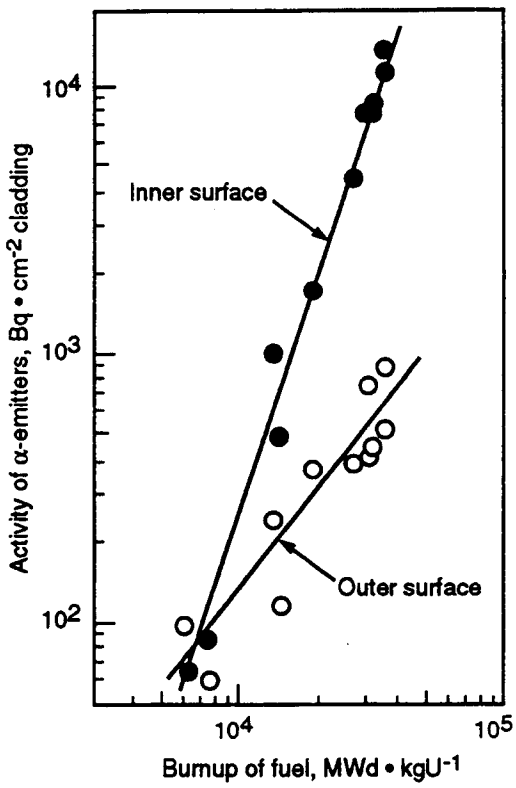

Figure 4-1. Gross activities of α emitters on the cladding surfaces as a function of fuel burnup (Hirabayashi et al., 1991)

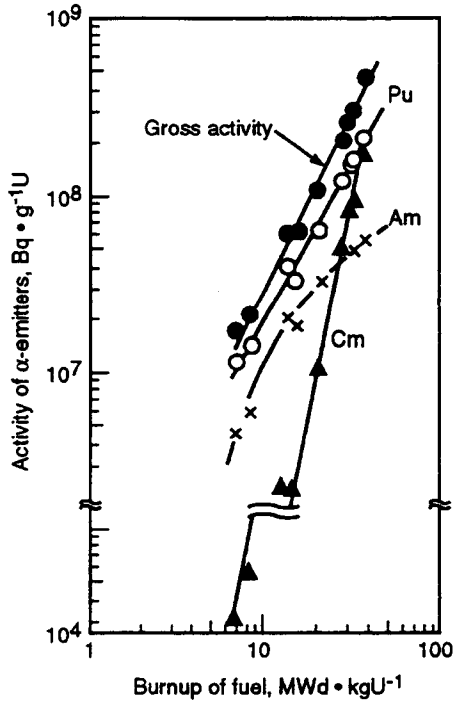

Figure 4-2. Elemental contribution to α activity in the spent nuclear fuel as a function of fuel burnup (Hirabayashi, et al., 1991)

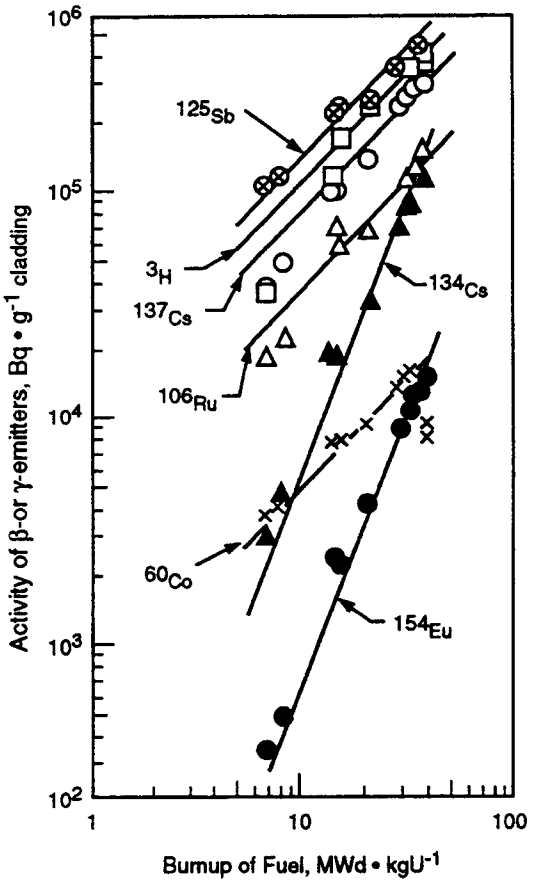

Figure 4-3. Activity of β or γ emitters in the spent fuel claddings (Hirabayashi, 1991)

layers of the cladding. The average concentration was found to be about 2 kBq $\cdot$ g^{-1} (about 50 nCi $\cdot$ g^{-1}) in the interior of cladding. Very limited leaching data on spent fuel cladding are available. In one of the studies, the leaching behavior of Zircaloy cladding from spent PWR fuel was investigated (Brodda and Merz, 1984). Two types of Zircaloy cladding with different pretreatments were available for experimental studies. The major characteristics of the two types of cladding specimens are given in Table 4-4. The specimens were boiled in a reflux condenser for 3 hours using 50 mL of the solutions. The solutions were filtered after cooling and their radioactive inventories measured. Double distilled water (H_2O), 7 M HNO_3, 1 M NaOH, Portland cement (PC) solution, alumina cement (AC) solution, and Sorel cement (SC) solution were used as leachants. The leached fraction was determined for six γ-emitting isotopes and two actinides. Table 4-5 shows the results, in terms of the percent leached, for the γ-emitting nuclides. It is evident that the soluble species, Cs, dissolves relatively well in both alkaline and acidic solvents, in contrast to other elements studied. Table 4-6 gives the initial levels of the actinides ^{239}Pu, ^{240}Pu, and ^{244}Cm and their behavior under successive leaching with HNO_3, NaOH, and $K_2S_2O_7$. Figure 4-4 shows the radionuclide distributions within the Zircaloy cladding for the experimental series. The results are divided into 3 groups: (i) the actinides that are concentrated in a thin surface layer, (ii) the diffusing species, whose highest concentration is in the inner surface layer but which also penetrate deeper into the material, and (iii) the activation products that are, partly, located on the external surface as corrosion products, but which otherwise display a homogeneous distribution.

Table 4-2. Distribution of the main β and γ emitters in spent fuel cladding with 29.4 MWd · kgU^{-1} burnup and 5 years cooling (Hirabayashi et al., 1991)

Depth (μm)	Radioactivity (Bq · g^{-1} cladding)									
	^{3}H	^{60}Co	^{90}Sr	^{106}Ru	^{125}Sb	^{134}Cs	^{137}Cs	^{144}Ce	^{147}Pm	^{154}Eu
0 - 3.7	9.83×10^{7}	1.14×10^{6}	2.2×10^{9}	8.9×10^{8}	1.02×10^{8}	8.3×10^{8}	2.93×10^{9}	3.31×10^{8}	2.2×10^{9}	1.20×10^{8}
3.7 - 5.4	5.01×10^{7}	9.0×10^{5}	1.1×10^{9}	7.2×10^{8}	8.25×10^{7}	4.07×10^{8}	1.33×10^{9}	1.24×10^{8}	8.5×10^{8}	4.1×10^{7}
5.4 - 6.8	3.07×10^{7}	1.8×10^{6}	6.2×10^{8}	3.30×10^{8}	5.59×10^{7}	9.5×10^{7}	4.43×10^{8}	2.64×10^{7}	1.6×10^{8}	6.7×10^{6}
6.8 - 10	1.54×10^{7}	9.7×10^{5}	—	5.0×10^{7}	2.13×10^{7}	7.1×10^{6}	2.22×10^{7}	—	—	9.0×10^{5}
10 - 20	4.80×10^{7}	1.29×10^{6}	—	4.9×10^{6}	3.41×10^{7}	4.80×10^{6}	1.75×10^{7}	—	—	7.0×10^{5}
20 - 80	6.96×10^{7}	1.19×10^{6}	—	1.11×10^{6}	3.21×10^{7}	8.8×10^{5}	3.39×10^{6}	—	—	1.46×10^{5}
80 - 135	6.39×10^{7}	1.11×10^{6}	—	6.5×10^{5}	3.15×10^{7}	1.54×10^{5}	5.6×10^{5}	—	—	—
135 - 189	4.55×10^{7}	1.13×10^{6}	—	1.03×10^{6}	3.24×10^{7}	5.3×10^{4}	1.90×10^{5}	—	—	—
189 - 241	5.51×10^{7}	1.15×10^{6}	7.0×10^{7}	4.0×10^{5}	3.42×10^{7}	4.7×10^{4}	1.59×10^{5}	2.8×10^{6}	1.4×10^{7}	7.7×10^{5}
241 - 385	3.67×10^{4}	1.22×10^{6}	6.9×10^{4}	2.9×10^{5}	3.42×10^{7}	2.5×10^{4}	1.11×10^{5}	2.8×10^{4}	1.3×10^{5}	7.1×10^{5}
385 - 524	1.61×10^{7}	1.23×10^{6}	—	2.9×10^{5}	3.42×10^{7}	—	3.4×10^{4}	—	—	—
524 - 617	1.03×10^{8}	1.21×10^{6}	—	1.7×10^{5}	3.28×10^{7}	—	3.0×10^{4}	—	—	—
617 - 620*	7.41×10^{7}	1.59×10^{7}	8.9×10^{5}	6.3×10^{7}	1.45×10^{8}	9.0×10^{5}	1.58×10^{6}	4.2×10^{6}	3.9×10^{7}	2.5×10^{6}

* Outer surface layer

Table 4-3. Distribution of the main α emitters in spent fuel cladding with 29.4 MWd · kgU^{-1} burnup and 5 years cooling (Hirabayashi et al., 1991)

Depth (μm)	Radioactivity (Bq · g^{-1} cladding)					
	Gross α	U	Np	Pu	Am	Cm
0 - 3.7	1.97×10^{6}	1.6×10^{1}	6×10^{0}	9.7×10^{5}	3.93×10^{5}	5.12×10^{5}
3.7 - 5.4	3.6×10^{4}	4×10^{0}	$<4\times10^{0}$	1.48×10^{4}	7.43×10^{3}	8.7×10^{3}
5.4 - 6.8	3.03×10^{4}	$<1.6\times10^{0}$	$<5\times10^{0}$	1.38×10^{4}	4.7×10^{3}	7.6×10^{3}
6.8 - 10	7.6×10^{3}	—	—	—	—	—
10 - 20	8.7×10^{3}	—	—	—	—	—
20 - 80	3.5×10^{3}	—	—	—	—	—
80 - 135	2.06×10^{3}	—	—	—	—	—
135 - 189	1.52×10^{3}	—	—	—	—	—
189 - 241	1.47×10^{3}	—	—	—	—	—
241 - 385	1.39×10^{3}	$<5\times10^{-2}$	$<5\times10^{0}$	6.1×10^{1}	2.69×10^{2}	3.15×10^{2}
385 - 524	1.49×10^{3}	—	—	—	—	—
524 - 617	1.61×10^{3}	—	—	—	—	—
617 - 620*	2.20×10^{5}	5×10^{1}	$<2\times10^{0}$	1.45×10^{5}	2.60×10^{4}	3.33×10^{4}

* Outer surface layer

Table 4-4. Characteristics of cladding specimens investigated (adapted from Brodda and Merz, 1984)

Type	Specimen Identification	
	KWU (P-1)	WAK (P-2a and P-2b)
Initial enrichment	3.1%	3.02%
Burnup	30 MWd · kgU^{-1}	28.2 MWd · kgU^{-1}
Mean power density of fuel rod	180 W · cm^{-1}	200 W · cm^{-1}
Discharge from reactor	1977	1975
Reprocessing date	Not applicable	1977
Cladding hull material	Zircaloy-4	Zircaloy-4
Separation fuel-cladding hulls	Mechanical	Chemical

From that investigation, it can be concluded that there are two main sources of radioactivity. The first is surface contamination or surface nuclide implantation due to nuclear recoil effects—the observed leaching of various nuclides by different aqueous solvents indicates that the radioactivity must be, in part, pure surface contamination. However, some fraction is also firmly implanted in the oxide layer. Although the actinides, like the rare earths, display very low diffusion rates in Zircaloy, the opposite is true of some fission products. The depth distribution measured for Ru and Cs leads one to suppose that similar diffusion behavior may also be valid for other chemically related elements. It thus becomes clear that a surface decontamination of the Zircaloy cladding would almost completely eliminate the actinides but not all fission nuclides. The second source is activation products of the cladding, which are distributed fairly evenly through the thickness of the material—the radionuclides ^{60}Co and ^{125}Sb are characteristic of this group. Based on the results of the investigation, one could conclude that cement could improve the radionuclide leaching resistance—that is, that actinides cannot be put into solution by alkaline solvents and thus cannot be made mobile. Therefore, embedding the Zircaloy cladding in cement for disposal may be beneficial. Cement, however, does not contribute to permanently improving the leaching resistance of alkaline and alkaline earth elements nor, presumably, that of Ru. It may just delay their release.

In developing packaging concepts for Zircaloy clad spent fuels, the level of ^{3}H and ^{85}Kr may also play a role. Therefore, the generation of hydrogen gas by radiolysis, which can lead to an increase in tritium release, must also be taken into consideration in estimates of the distribution of the canister failures as a function of time. The ^{3}H is rather firmly bound into the Zircaloy matrix in the form of zirconium tritide and is released only at relatively high temperatures (800 to 1000°C). On the other hand, zirconium tritide exchanges its hydrogen isotopes in contact with aqueous solutions or hydrated solids, such as cement products. An isotope exchange process of this type can lead to an increased ^{3}H release from the cemented Zircaloy clad fuels. The behavior of the inert gas ^{85}Kr, which enters the Zircaloy cladding by means of recoil effects, is especially interesting. A mean ^{85}Kr inventory of 62 μCi per gram of Zircaloy was measured for PWR cladding with a burnup of 31 MWd·kgU^{-1} (Brodda and

Table 4-5. Percent release of γ-emitting nuclides from Zircaloy cladding specimens in different leachants (Brodda and Merz, 1984)

Hull Type	Nuclides	Initial Radioactivity ($\mu Ci \cdot g^{-1}$)	Radionuclide Leached (%)					
			H_2O	HNO_3	NaOH	PC	AC	SC
P-1	^{134}Cs	181	7.8	10.9	15.4	9.8	13.8	12.7
	^{137}Cs	936	7.2	11.0	14.9	9.9	13.8	12.7
	^{106}Rh	414	ND	21.4	1.1	ND	ND	1.7
	^{154}Eu	33	ND	0.4	ND	ND	ND	ND
	^{125}Sb	1234	0.8	2.3	3.5	0.2	0.9	0.5
	^{60}Co	69	ND	0.3	1.5	ND	ND	ND
P-2a	^{134}Cs	41	1.5	12.4	3.7	2.4	3.2	1.3
	^{137}Cs	498	1.5	12.5	3.7	2.3	3.0	1.4
	^{106}Rh	13	ND	99.5	1.8	NM	NM	NM
	^{154}Eu	14	ND	2.8	ND	ND	ND	ND
	^{125}Sb	222	0.9	30.2	7.7	0.1	1.0	1.8
	^{60}Co	26	ND	40.7	2.9	ND	ND	ND
P-2b	^{134}Cs	0.4	49.8	81.9	56.1	NM	NM	NM
	^{137}Cs	3.8	75.8	95.6	86.1	NM	NM	NM
	^{106}Rh	2.5	24.0	99.5	2.7	NM	ND	NM
	^{154}Eu	ND	ND	ND	ND	ND	ND	ND
	^{125}Sb	45	23.2	28.3	10.3	ND	28.0	NM
	^{60}Co	8	9.1	48.4	4.3	NM	ND	NM

ND = Not Detectable
NM = Not Measured
PC = Portland Cement solution
AC = Alumina Cement solution
SC = Sorel Cement solution

Table 4-6. Percent release of actinides from Zircaloy cladding specimens in different leachants (Brodda and Merz, 1984)

Hull Type	Initial Radioactivity ($\mu Ci \cdot g^{-1}$)		Successive Order of Leachant Use	Leached Amount (%)	
	$^{239,240}Pu$	^{244}Cm		$^{239,240}Pu$	^{244}Cm
P-1	150	260	HNO_3	60	46
			$K_2S_2O_7$	40	54
			NaOH	ND	ND
			$K_2S_2O_7$	57	52
P-2a	1100	570	HNO_3	90	40
			$K_2S_2O_7$	10	60
			NaOH	ND	ND
			$K_2S_2O_7$	59	100
P-2b	440	10	HNO_3	98	100
			$K_2S_2O_7$	2	ND
			NaOH	ND	ND
			$K_2S_2O_7$	70	80

ND = Not Detectable

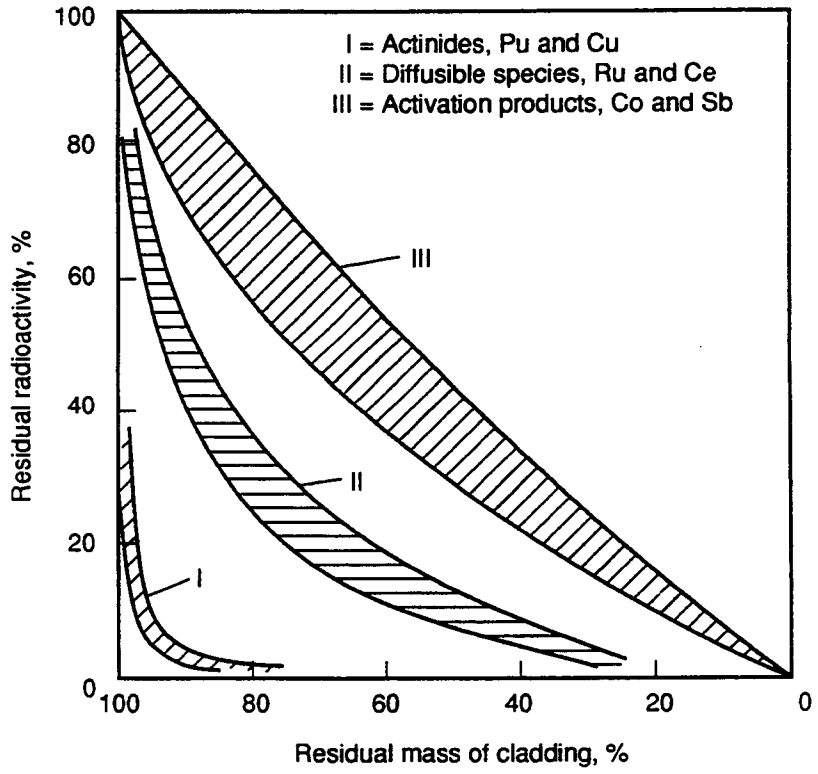

Figure 4-4. Radionuclide distributions in Zircaloy cladding specimens (Brodda and Merz, 1984)

Merz, 1984). This corresponds to approximately 0.1 percent of the total inventory in the fuel rod. It has also been shown that the ^{85}Kr activity is almost completely restricted to the inner corrosion layer of the cladding tubes, which is approximately 10 μm thick.

4.2 RADIOACTIVITY IN SPENT FUEL

When fuel is irradiated in a reactor, three general groups of radioisotopes are formed: (i) fission products, (ii) actinides, and (iii) activation products. More than 350 nuclides have been identified as fission products, many of them with very short half-lives. The exact quantities depend on the irradiation history of the fuel and the time after discharge. The concentration of any isotope can be computed, in principle, using the following differential equation, Eq. (4-1) (Tsoulfanidis and Cochran, 1991):

$$dN_i/dt = \sum_{j=1}^{N} l_{ij}\,\lambda_j\,N_j + \phi \sum_{k=1}^{N} f_{ik}\,\sigma_k\,N_k - \left(\lambda_i + \phi\,\sigma_i + r_i\right) N_i + F_i \mid i = 1, M \qquad (4\text{-}1)$$

where

N_i = atom density of nuclide i

M = number of nuclides in the chain containing nuclide i

l_{ij} = fraction of decays of nuclide j leading to the formation of species i

λ_i = radioactive decay constant of species i

ϕ = position and energy-averaged neutron flux

f_{ik} = fraction of neutron absorption by nuclide k leading to formation of species i

σ_k = average neutron absorption cross section of nuclide k

r_i = continuous removal rate of nuclide i from the system

F_i = continuous feed rate of nuclide i; if nuclide i is produced by fission, $F_i = Y_i \Sigma f_{ik} \phi$, where Y_i = fission yield of nuclide i.

Equation (4-1) is not linear if either the flux, ϕ, or any of the cross sections are functions of time. The activity of the nuclides produced by the activation of Zr in the cladding and of Ni and Co isotopes found in the steel used in control rods and in fuel assembly spacer grids should be added to the activity from fission products and actinides.

To calculate the total activity in spent fuel as a function of time, Eq. (4-1) must be solved for all isotopes of interest and the results summed. A widely used code that performs this task is ORIGEN (Croff, 1983; Bell, 1973; Klein, 1987; Bowman, 1992). Analytical fits for ORIGEN code have been

developed to give the activity as a function of time after discharge (Locke, 1975). The calculations of the code have been validated against experimental data on spent fuel radionuclide inventories (Heeb et al., 1990).

4.3 CHARACTERISTICS OF SPENT FUEL

Irradiated fuel still contains most of its original ^{238}U, about one-third of its original ^{235}U, almost all the fission products, all the transuranic (TRU) isotopes, and many activation products. Tables 4-7 and 4-8 summarize the most important isotopic features of typical LWR spent fuels. The volume of wastes generated during the service life of LWRs is given in Table 4-9.

4.4 STORAGE OF SPENT LWR FUEL

Prior to permanent disposal in a repository, the spent fuel is expected to be stored for some years (perhaps 10 years or more) to allow the assemblies to cool down as a result of dissipation of the decay heat. Two principle methods are available for storing the spent fuel for extended periods of time, namely, wet storage in water pools and dry storage in air or gases (EPRI, 1986; Bailey et al., 1986; EPRI, 1984; Johnson, 1979). Water pool storage has been used in the U.S. since the first reactors were built in 1943 (Johnson, 1977). However, experience with dry storage, an alternative to extended wet storage, is rather limited. The fuel may be stored unconsolidated or consolidated. By definition, unconsolidated fuel means intact assemblies; consolidated means the fuel rods are removed from the fuel assembly and placed in a grid with closer spacing than that of an intact assembly, or the rods are placed in a close-packed array inside a canister (Zacha, 1988; Johnson, 1986; EPRI, 1989). Volume savings of 2:1 by consolidation have been demonstrated by many utilities (Zachy, 1988). The advantages of fuel rod consolidation are obvious: (i) storage capacity would be almost doubled, and (ii) the number of spent-fuel shipping casks can be halved.

In the wet storage mode, the decay heat from the spent fuel is removed by deionized water (DIW) at a temperature below 40°C. Zircaloy cladding does not experience any significant additional corrosion or hydriding under such conditions compared to that experienced while in core. In the dry storage mode, the decay heat is removed by using air or an inert gas (usually helium or nitrogen) under forced convection. The dry storage facility is simpler and cheaper to maintain compared to wet storage. On the other hand, the dry environment has the potential of producing such problems as further fuel cladding oxidation, increased cladding stresses and creep deformation as a result of rod internal pressure, and volume expansion of the fuel due to air permeating through any pinholes and incipient cracks in the cladding. These possible spent fuel and cladding alteration modes could be quite accelerated under dry storage conditions, since the temperatures are much higher than in wet storage. Temperatures in the range of 300 to 400°C are being considered for the extended dry storage of spent fuel for periods up to 100 years following discharge from the reactor. Because of the stated reasons, any extended dry storage may require evaluation of any additional process of materials degradation or alteration of the cladding properties which may influence its subsequent behavior in a repository. Long-term behavior of extended wet stored spent fuel may need to be modeled differently from assemblies that experience dry storage following discharge from the reactor.

Allowable long-term storage temperatures and times for dry storage of spent LWR fuels will depend upon a number of factors including cladding stress levels, fuel type and assembly design, materials condition of the cladding at the time of discharge, decay heat history of the spent fuel, and heat

Table 4-7. Radioactivity from principal fission products in irradiated fuel* (Tsoulfanidis and Cochran, 1991)

Nuclide	Half-life	Activity per year (1×10^6 Ci) (at discharge)
^{3}H	12.4 y	1.93×10^{-2}
^{85}Kr	10.76 y	0.308
^{90}Sr	27.7 y	2.11
^{95}Zr	65.5 d	37.3
^{106}Ru	368 d	14.8
^{125}Sb	2.71 y	0.237
^{129}I	1.7×10^7 y	1.01×10^{-6}
^{131}I	8.05 d	23.5
^{133}Xe	5.27 d	43.9
^{134}Cs	2.046 y	6.7
^{137}Cs	30.0 y	2.94
^{144}Ce	284 d	30.2
^{151}Sm	87 y	3.41×10^{-2}
^{154}Eu	16 y	0.191
^{155}Eu	1.81 y	0.204

* The fuel is assumed to be from a 1000-MW (electric) PWR, with an initial enrichment 3.3% in ^{235}U and operated for 3 y with an 80% capacity factor.

dissipation capacity of the storage installation. A recent investigation of the potential failure modes of Zircaloy fuel cladding during dry storage, covering stress/creep rupture, stress corrosion cracking (SCC), and cladding rupture due to delayed hydride cracking (DHC), has identified stress/creep rupture as the likely dominant failure mode (Gilbert et al., 1990). The internal pressure from helium and fission gases within the fuel rods are the sources that may lead to such a failure, if pressures and temperatures are sufficiently high. However, another study concluded that spent PWR fuel can be stored safely for a period of 1,000 years under dry storage conditions at a temperature of 400°C (Einziger et al., 1982).

4.4.1 U.S. Spent Fuel Inventory

The oldest BWR spent fuel currently in storage was discharged in 1968, whereas the oldest PWR spent fuel in storage was discharged in 1970 (U.S. DOE, 1982). Spent fuel discharged in prior

Table 4-8. Radioactivity from principal actinides in irradiated fuel* (Tsoulfanidis and Cochran, 1991)

Nuclide	Half-life (y)	Activity per year (Ci)	Mass or Concentration (kg · kgU^{-1})
^{234}U	2.47×10^{5}	19.4	0.12×10^{-3}
^{236}U	2.39×10^{7}	7.22	4.18×10^{-3}
^{237}Np	2.14×10^{6}	14.4	0.75×10^{-3}
^{236}Pu	2.85	134	9.20×10^{-9}
^{238}Pu	86	1.01×10^{5}	0.22×10^{-3}
^{239}Pu	24,400	8.82×10^{3}	5.28×10^{-3}
^{240}Pu	6,580	1.30×10^{4}	2.17×10^{-3}
^{241}Pu	13.2	2.81×10^{6}	1.02×10^{-3}
^{242}Pu	3.79×10^{5}	37.6	0.35×10^{-3}
^{241}Am	458	4.53×10^{3}	0.05×10^{-3}
^{243}Am	7,950	477	0.09×10^{-3}
^{242}Cm	163 d	4.40×10^{5}	4.90×10^{-6}
^{244}Cm	17.6	7.38×10^{4}	3.30×10^{-5}

* Fuel burnup is 33 MWd · kgU^{-1} in a 1000-MW (electric) PWR, and 150 days after discharge.

years has been reprocessed. The total inventory of LWR spent fuel in storage in the U.S. as of the end of 1990, was 77,398 assemblies. These assemblies represent initial U content of approximately 22×10^{6} kg, of which 38 percent are from BWRs and 62 percent are from PWRs (U.S. DOE, 1992b). Table 4-10 shows the inventory breakdown for BWR and PWR spent fuel discharged from 1968 through 1990 (U.S. DOE, 1992b). Annual spent fuel discharges and fuel burnup are shown in Table 4-11. The majority of spent fuel is stored in water in storage pools at reactor sites, but there are 404 assemblies in dry storage (U.S. DOE, 1992b). Of the 114 reactors expected to be in operation in the year 2000, as many as 26 reactors appear to require expansion above current pool maximums prior to the year 2000. The current inventory of the spent fuel assemblies represents less than one-third of the spent fuel scheduled for disposal in the first geologic repository in the United States.

A computerized database, called the Characteristics Data Base (CDB), is currently available which provides additional information about the discharged fuel assemblies (U.S. DOE, 1988a; 1988b; Notz et al., 1992). Another database that provides the quantities of spent fuel, radioactive waste inventories, and projections for high-level, low-level, and transuranic wastes both from the commercial

Table 4-9. Lifetime radioactive waste generation from a PWR and a BWR* (adapted from Tsoulfanidis and Cochran, 1991)

Waste Type	Reference PWR, 1000 MW (electric)		Reference BWR, 1000 MW (electric)	
	Volume (m^3)	Radioactivity (undecayed curies)	Volume (m^3)	Radioactivity (undecayed curies)
Once-through fuel cycle wastes				
Mill tailings	4.353E+06 [a]	3.710E+03	4.867E+06	4.149E+04
LLW from uranium conversion [b]	3.411E+02	9.813E+03	3.814E+02	1.097E+04
LLW from uranium enrichment [c]	1.328E+02	9.716E+03	1.365E+02	1.080E+04
LLW from fuel fabrication	3.063E+03	7.288E+00	4.110E+03	9.781E+00
LLW from reactor power generation	3.032E+04	2.866E+04	5.217E+04	7.956E+04
Reactor spent fuel	5.213E+02	3.270E+09 [d]	6.996E+02	3.342E+09 [d]
Decommissioning wastes				
LLW	1.510E+04	1.057E+05	1.640E+04	2.532E+05
Greater than Class C wastes	1.130E+02	4.070E+06	4.070E+01	5.300E+06
TOTAL	4.403E+06	3.274E+09	4.941E+06	3.348E+09

* Waste generated from 40 y of reactor operation and 26,000 MW (electric) • y

[a] Read as 4.353×10^6

[b] Applies to the fluorination/fractionation process

[c] Applies to the gaseous diffusion process

[d] Based on activity levels measured 1 y after reactor discharge. For the PWR, these levels are based on a burnup of 33 MWd • kgU^{-1}. Activity levels for the BWR are based on a burnup of 27.5 MWd • kgU^{-1}.

Table 4-10. Spent fuel discharged during 1968-1990 from commercial LWRs in the United States (U.S. DOE, 1992b)

Reactor Type	Number of Assemblies		
	Stored at Reactor Site	Stored at Off-Site Storage Facility	Total
BWR	42,338	2,955	45,293
PWR	31,612	493	32,105
TOTAL	73,950	3,448	77,398
	Amount of Uranium (kg $\times 10^{-3}$)		
BWR	7,673.1	553.9	8,227.0
PWR	13,494.8	192.5	13,687.3
TOTAL	21,167.9	746.4	21,914.3

and defense activities is also available (Klein, 1987). This database, called the Integrated Data Base (IDB), provides updated projections of the wastes in the U.S. through the year 2020. The information available in the CDB includes the details about the physical, radiological, and quantitative characteristics of the spent fuel organized by assembly class, type codes, length and width of the assemblies and individual fuel rods, number of fuel rods, type of material used for cladding, and other parts of the assembly. The radiological characteristics have been generated using ORIGEN code (Parks, 1992; Welch et al., 1990; Welch and Notz, 1990). Included in the database is the information related to the burnup and number of damaged and leaking assemblies (U.S. DOE, 1992a). The summary of data related to defective BWR and PWR spent fuel assemblies, as of the end of 1988, is shown in Tables 4-12 and 4-13, respectively (Moore et al., 1990). These data clearly show high defect rates for certain assembly designs. As shown in Table 4-10, GE Model 2, 7 $\times$ 7 fuel design assemblies operated in GE Model 2/3 BWRs show spent-fuel defects in 1469 out of 6719 assemblies, with a defective rate of 21.9 percent. The same design assemblies for GE Model 4/5/6 BWRs show 385 defective assemblies out of 1142 irradiated assemblies, with a rate as high as 33.7 percent. One conclusion that can be drawn from the data is that operating/service and the type of reactor could have some influence on the condition of the assemblies at discharge. Discharged assembly defect rates for PWR assemblies, as shown in Table 4-11, are much lower. Although, modern day assemblies show practically zero defect rates, the number of defective discharged assemblies is quite high. This may require a well planned strategy for their disposal, and may require a different computation treatment for the source-term modeling of waste packages containing defected/leaker assemblies.

Pool-side fuel examinations and fission gas release data indicate that nearly 2,300 assemblies have failed or have damaged fuel rods (Gilbert et al., 1990). The total number of fuel rods with failed cladding is not known precisely. On the basis of visual observations and radiation monitoring of the pool water, it has been demonstrated that no significant degradation of Zircaloy cladding occurs during pool

Table 4-11. Spent fuel burnup and annual discharged quantities (adapted from U.S. DOE, 1992b)

Year	Number of Assemblies			kgU ($\times 10^3$)			Average Burnup (MWd • kgU^{-1})			
							All Discharged Assemblies		Equilibrium Cycle Discharges	
	BWR	PWR	Total	BWR	PWR	Total	BWR	PWR	BWR	PWR
1968	5	0	5	0.6	0.0	0.6	1.6	0.0	1.6	0.0
1969	96	0	96	9.8	0.0	9.8	15.2	0.0	15.2	0.0
1970	29	99	128	5.6	39.0	44.6	0.3	18.4	0.0	0.0
1971	408	113	521	64.0	44.5	108.5	5.8	23.9	16.6	0.0
1972	771	282	1,053	141.5	99.9	241.4	6.4	21.9	16.3	28.0
1973	577	165	742	95.2	67.1	162.3	12.4	23.7	15.9	28.1
1974	1,314	575	1,889	244.6	207.7	452.3	12.7	18.9	14.5	25.7
1975	1,224	797	2,021	225.7	321.8	547.5	16.9	18.1	17.3	27.3
1976	1,663	931	2,594	297.1	401.0	698.1	13.4	22.2	16.7	25.8
1977	2,047	1,107	3,154	382.9	466.9	849.8	16.6	25.1	19.0	27.8
1978	2,239	1,666	3,905	383.2	699.0	1,082.3	19.8	26.4	22.1	28.7
1979	2,131	1,664	3,795	399.8	722.1	1,121.9	22.4	27.0	23.7	30.2
1980	3,330	1,456	4,786	619.9	618.1	1,237.9	22.4	29.7	23.3	30.7
1981	2,467	1,585	4,052	458.7	675.9	1,134.6	23.9	30.2	23.9	30.9
1982	1,951	1,493	3,444	357.2	641.3	998.5	24.7	29.7	24.9	32.3
1983	2,698	1,780	4,478	491.3	773.1	1,264.5	26.7	30.0	26.7	31.6
1984	2,736	1,951	4,687	498.0	847.6	1,345.7	25.4	29.4	25.4	32.0

Table 4-11. Spent fuel burnup and annual discharged quantities (adapted from U.S. DOE, 1992b) (cont'd)

Year	Number of Assemblies			kgU ($\times 10^3$)			Average Burnup (MWd • kgU^{-1})			
							All Discharged Assemblies		Equilibrium Cycle Discharges	
	BWR	PWR	Total	BWR	PWR	Total	BWR	PWR	BWR	PWR
1985	2,810	2,056	4,866	510.1	870.0	1,380.0	23.3	31.8	25.8	33.2
1986	2,551	2,348	4,899	458.2	1,022.5	1,480.6	21.0	30.4	27.3	33.7
1987	3,876	2,694	6,570	699.4	1,153.1	1,852.6	19.2	31.1	27.0	34.4
1988	2,957	2,731	5,688	535.8	1,162.5	1,698.2	24.1	33.0	27.0	35.3
1989	3,924	2,879	6,803	714.9	1,256.2	1,971.2	22.0	32.2	27.3	36.6
1990	3,486	3,594	7,080	633.0	1,552.2	2,185.2	25.0	33.8	27.8	35.8
Temps [a]	3	139	142	0.5	45.7	46.2	0.0	27.0	—	27.0
TOTAL	45,293	32,105	77,398	8,227.0	13,687.3	21,914.3	21.3	29.7	24.2	32.4

[a] Temps are temporarily discharged assemblies, as of December 31, 1990.

Table 4-12. Defective BWR fuels by assembly class and fuel design (Moore et al., 1990)

Fuel Assembly Design	GE BWR/2,3 (9 reactors)			GE BWR/4,5,6 (28 reactors)		
	Discharged Assemblies	Defective Assemblies	Percent Defective	Discharged Assemblies	Defective Assemblies	Percent Defective
GE Model 2 7 × 7 Fuel	6719	1469	21.9	1142	385	33.7
GE Model 3 Improved 7 × 7 Fuel	394	7	1.78	4936	130	2.63
GE Model 4 Original 8 × 8 Fuel	3876	1	0.03	3571	185	5.18
GE Model 5 8 × 8 Retrofit Fuel	792	1	0.13	3455	104	3.01
GE Prepressurized Fuel	1836	0	0.00	6591	144	2.18
GE Barrier Fuel	248	0	0.00	775	1	0.13
ANF 7 × 7 Fuel	260	0	0.00	Not Applicable		
ANF 8 × 8 Fuel	684	0	0.00	Not Yet Discharged		

GE — General Electric Company
ANF — Advanced Nuclear Fuel

Table 4-13. Defective PWR fuels by assembly class and fuel design (Moore et al., 1990)

Fuel Assembly Design	WE 14 × 14 (6 reactors)			WE 15 × 15 (10 reactors)			WE 17 × 17 (33 reactors)		
	Discharged Assemblies	Defective Assemblies	Percent Defective	Discharged Assemblies	Defective Assemblies	Percent Defective	Discharged Assemblies	Defective Assemblies	Percent Defective
WE Standard	592	1	0.2	1457	103	7.1	Not Applicable		
WE LOPAR	1409	77	5.5	3087	16	0.5	5102	99	1.9
WE OFA	88	1	1.1	266	1	0.4	628	1	0.2
WE VANTAGE 5	Not Yet Discharged			Not Yet Discharged			4	0	0.0
ANF for WE	559	0	0.0	743	12	1.6	139	0	0.0
ANF TOPROD	299	1	0.3	Not Applicable			Not Applicable		

WE — Westinghouse Electric Corporation
ANF — Advanced Nuclear Fuel

storage (Johnson, 1979; Johnson, 1977; Zima, 1979; Bradley et al., 1981; Bailey and Tokar, 1982). However, conclusions about the likely performance of the cladding in a geological repository cannot be made from wet storage observations, since the conditions are quite different. On the other hand, conditions experienced in dry storage could yield information relevant to a repository situation because of similarities between the two environments. However, experience and quantitative data accumulated for the dry storage of spent fuel is limited.

5 POST-DISCHARGE SPENT FUEL DEGRADATION

5.1 SPENT FUEL OXIDATION

Upon breach of the waste package and failure of the fuel cladding, the spent fuel will be exposed to the repository environment—which during the early stages is expected to be dry or contain moist air at elevated temperatures ranging from 250 to 100°C. Under the anticipated conditions in an unsaturated repository, it can be expected, thermodynamically, that the UO_2 fuel will oxidize completely to UO_3. The sequence of oxidation is believed to be $UO_2 \rightarrow U_4O_9 \rightarrow U_3O_7 \rightarrow U_3O_8 \rightarrow UO_3 \rightarrow UO_3 \cdot 2H_2O$ (Einziger, 1991). An uncertainty in modeling the long-term performance arises from the kinetics of the process.

The oxidation state of UO_2 spent fuel after an extended residence in a moist air atmosphere at elevated temperatures will affect the structural integrity of the fuel rod and the leaching characteristics of the fuel pellets. As long as the fuel retains its cubic structure, the primary concern is the change in leaching rate as the O/M ratio increases. If low density phases such as U_3O_8 form, then additional phenomena must be considered: (i) release of a large fraction of fuel matrix ^{85}Kr and ^{14}C inventory as gases, (ii) spallation of fuel into powder, increasing the surface area available to a leachant, and (iii) stress from swelling fuel that is likely to split the cladding, thus decreasing the length of the flow path of the leachant to and from the fuel. The extent to which these effects may appear would depend on the oxide phases present in the fuel.

Studies of spent fuel indicate that oxidation proceeds by forming U_4O_9 along grain boundaries and by subsequent growth of the U_4O_9 into the individual UO_2 grains (Woodley et al., 1989; Einziger et al., 1991). The oxidation of spent fuel differs from unirradiated UO_2 both in its rapid penetration along grain boundaries and in the formation of a different oxidation product. An experimental investigation reported in the literature used four LWR fuels that covered a range of burnup, grain size, and fission gas release, as shown in Table 5-1. The weight gains at 195°C due to oxidation in moist air are shown by the increase in the O/M ratio in Figure 5-1. Table 5-2 ranks the fuels by relative initial weight gain and lists some parameters, such as grain size, fission gas release, burnup, and fuel type, that are commonly thought to affect oxidation rate. No simple correlation is apparent from these results.

The examination of spent fuels used in the investigation confirmed that oxidation occurred by the formation and growth of U_4O_9 along the original UO_2 grain boundaries (Einziger et al., 1992). The oxidation behavior observed in low gas-release fuels (ATM-105, ATM-104, and Turkey Point) consisted of uniform grain boundary oxidation extending from near the pellet outer edge to near the mid-radius. Oxidized fuel particles from near the pellet centers in low-gas release fuels exhibited localized oxidation around the particle surfaces. In high-gas release fuel (ATM-106), uniform grain boundary oxidation occurred in samples which were from regions near the fuel pellet center. The reasons for this difference in oxidation are not understood, but are believed to be related to the fuel microstructure formed during burnup.

5.1.1 Fuel Condition Dependence

The O/M ratio versus time data shown in Figure 5-1 vary initially by as much as a factor of four between fuels. However, the shape of these O/M ratio curves appear quite similar after a relatively short period of time. This is demonstrated in Figure 5-2a (Einziger et al., 1992) by the rate of O/M

Table 5-1. Fuel specimen characteristics (adapted from Einziger et al., 1991)

Properties/Parameters	ATM-105 Cooper	Turkey Point	ATM-104 Calvert Cliffs	ATM-106 Calvert Cliffs
Fuel type	BWR 7 × 7	PWR 15 × 15	PWR 14 × 14	PWR 14 × 14
Nominal burnup, MWd • kgU^{-1}	28	27	43	48
Fission gas release, %	0.6	<0.3	1.1	18
Initial enrichment, wt. % ^{235}U	2.93	2.56	3.04	2.45
Initial pellet density, % of theoretical	95	92	94 to 96	92 to 94
Postirradiation grain size, μm	11 to 15	20 to 30	10 to 13	7 to 15
Average nominal LHGR kW • m^{-1}	17	18.2	21	NA
Postirradiation cooling time, yr	8.7	15.3	8.7	10.3

NA: Not available
ATM: Approved Testing Material

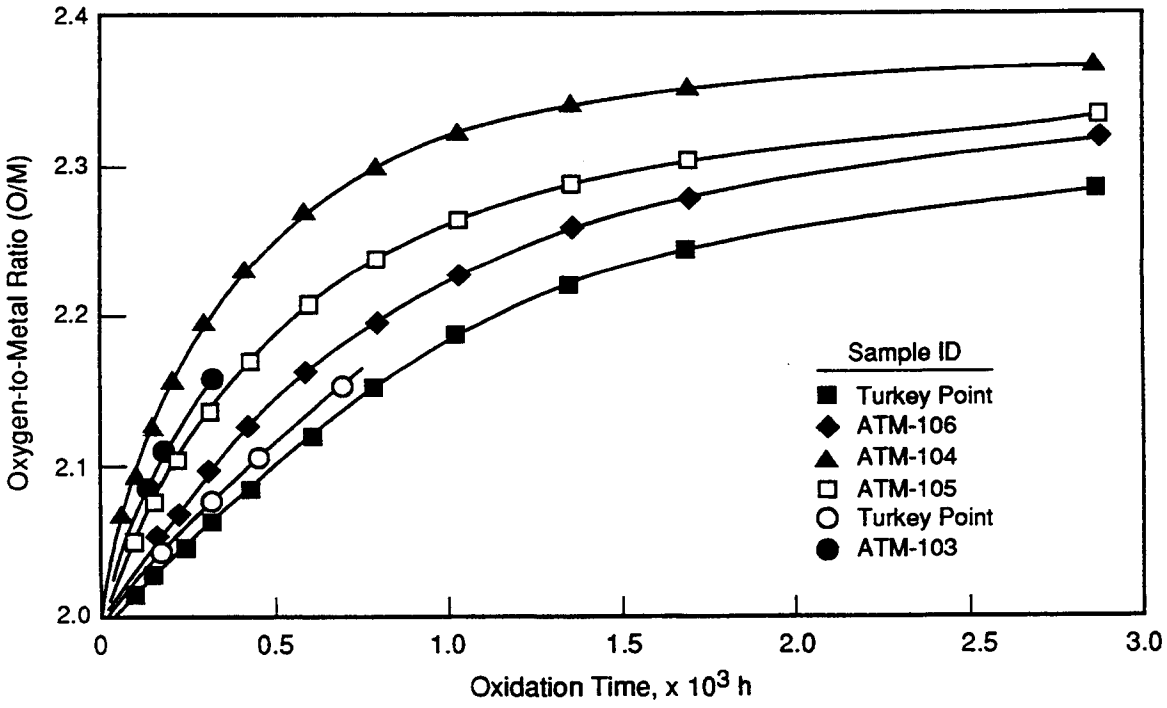

Figure 5-1. O/M ratio with oxidation time in flowing dry air at 195°C (Einziger et al., 1992)

Table 5-2. Ranking of fuels by weight gain (adapted from Einziger et al., 1992)

Specimen Identification [a]	Grain Size, μm	Gas Release, %	Fuel Type	Approximate Burnup, MWd · kgU^{-1}
104	5-15	1.1	PWR	43
[105	11-15	0.6	BWR	28
[103	18.5	0.3	PWR	30
[106	10-13	18	PWR	48
[TP	20-30	<0.3	PWR	27

[a] Weight gain in descending order. Bracket indicates essentially equal weight gain.
TP: Turkey Point fuel

change, d(O/M)/dt, as a function of time. Although it is reported that after a short time (approximately 500 hours at 195°C and 2000 hours at 175°C) the d(O/M)/dt becomes essentially independent of fuel type, this conclusion is not supported by the data presented. However, it is clear from Fig. 5-2a that the rate of oxidation for all test samples reduces substantially with increasing time. Figure 5-2b shows the spent-fuel oxidation data for exposure up to 3000 hours. From the graphs, it is clear that the rate of oxidation of the different spent-fuel samples test varies by as much as a factor of 10, even after 3000 hours of oxidation. The oxidation curves also cross after approximately 600 hours of exposure. After a few thousand hours at 175°C, d(O/M)/dt is reported to be the same for BWR fuel of average grain size oxidized at a dewpoint of 80°C, and large-grained PWR fuel oxidized at dew points of −55°C and 80°C (factor of approximately 10^5 in moisture content). The observation is based on tests that have run for ~30,000 hours (Einziger et al., 1992). From this observation, one would conclude that the oxidation rate is independent of the moisture content. This fact could be of considerable significance in reducing the impact of some of the uncertainty related to possible changes in the moisture content of the unsaturated repository over the long period of regulatory interest.

5.1.2 Temperature Dependence

As shown in Figures 5-1 and 5-2, after a peak, d(O/M)/dt rapidly decreases with time, and the O/M ratio approaches a saturation plateau between 2.35 and 2.4 at 195°C. Longer term oxidation tests at 250 and 175°C indicate an O/M ratio value closer to 2.4 (Einziger and Strain, 1986). U_4O_{9+x} is the only observed phase at this O/M ratio. However, tests at higher temperatures indicate that this may be only a quasi-equilibrium O/M ratio, and eventually oxidation to a higher state may occur. These observations are combined to generate a universal O/M ratio curve, as shown schematically in Figure 5-3. The data indicate that there is a minimum time given by $t_{2.4}+\delta$, which is a function of temperature, before detrimental lower density phases, such as U_3O_8, form (Einziger et al., 1992). Currently, it is not known why a plateau in the O/M ratio curve of Figure 5-3 occurs or if any mechanistic changes take place in the fuel while it is on the plateau (Einziger et al., 1992). Since δ was at least 9000 hours at 250°C for U_4O_{9+x} to transform to U_3O_8, it is expected that the time for a higher phase such as U_3O_8 to form at lower temperatures would be greatly extended, assuming an Arrhenius dependence.

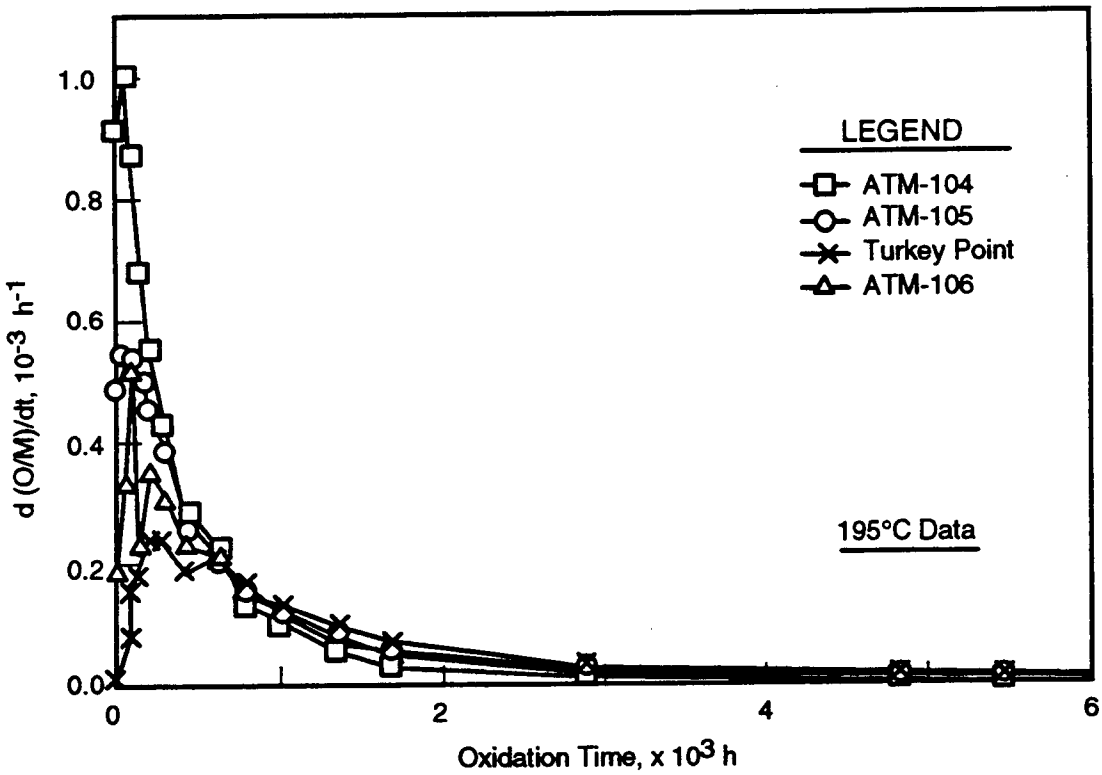

Figure 5-2a. Time rate of change in O/M ratio as a function of oxidation time up to 5500 hours (Einziger et al., 1992)

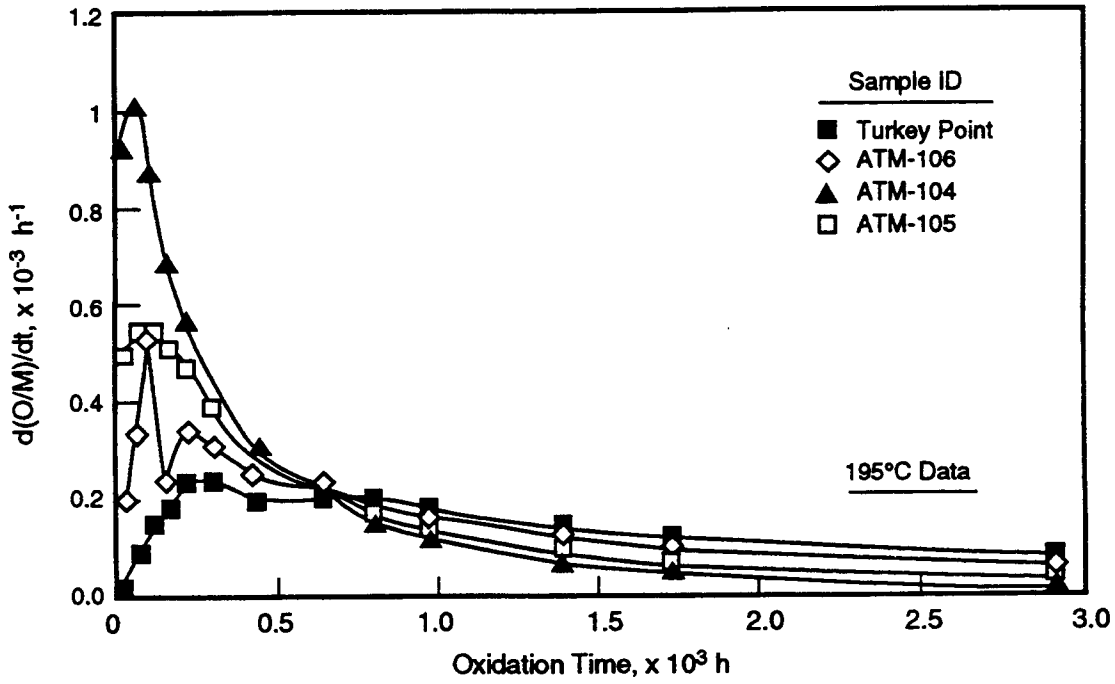

Figure 5-2b. Time rate of change in O/M ratio as a function of oxidation time up to 3000 hours (Einziger et al., 1992)

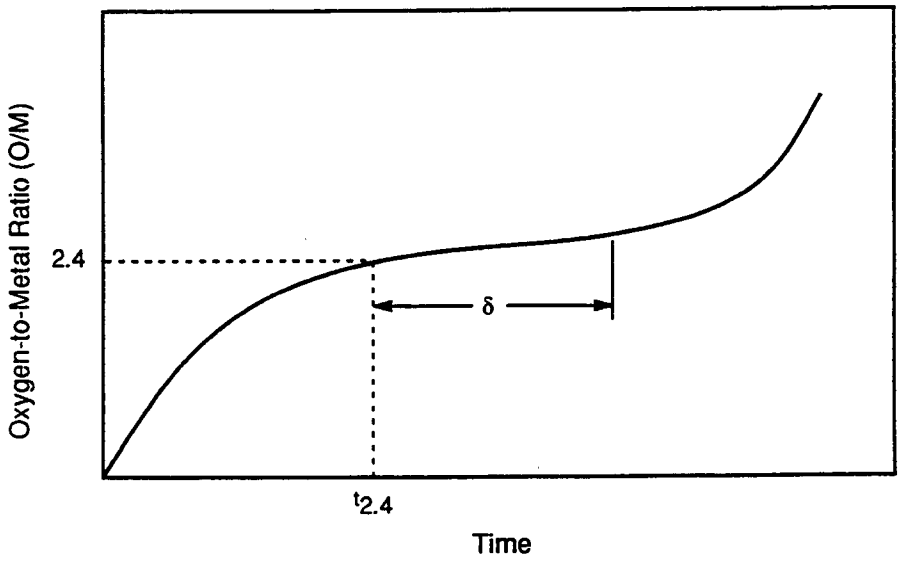

Figure 5-3. Schematic of O/M ratio in spent fuel as a function of oxidation time (Einziger et al., 1992)

The growth exhibits parabolic kinetics. Extrapolation of the oxidation rate indicates that the U_4O_9 will remain stable for a period longer than 2000 years at 95°C (Einziger et al., 1992).

5.1.3 Spent Fuel Corrosion and Degradation

In a recently reported detailed investigation on the leaching behavior of spent UO_2 fuel, test samples from both BWR and PWR fuels were used. The fuel/clad samples had a maximum burnup of approximately 40 $MWd \cdot kgU^{-1}$ (Forsyth and Werme, 1992). As shown in Table 5-3, two aqueous leachants, namely, a synthetic groundwater (SGW) and DIW, were used. All tests were performed at temperatures in the range of 20 to 25°C. The results of the investigation are summarized below.

Table 5-3. Composition ($mmol \cdot L^{-1}$) of SGW at pH of 8.0-8.2 (Forsyth and Werme, 1992)

Na^+	K^+	Mg^{2+}	Ca^{2+}	Si	HCO_3^-	Cl^-	SO_4^{2-}
2.8	0.1	0.2	0.45	0.2	2.0	2.0	0.1

5.1.4 Oxic Conditions

Oxic conditions are likely to be present, at least during the early part of the isolation period, in the geologic repository site currently being investigated in the United States. Therefore, understanding of the kinetics of release of actinides and fission products under such conditions is of interest.

5.1.4.1 Release of Actinides

The data on the concentration of U released in the two types of water are plotted against the cumulative contact time in Figure 5-4. In the first week of contact with the SGW, the concentration increases to 5×10^{-6} mol$\cdot$L^{-1} and remains at that approximate level for 1000 days. At longer times, there appears to be a slowly increasing trend in concentration. For DIW, the U concentrations are lower, generally around 1×10^{-7} mol$\cdot$L^{-1}. The Pu data are shown in Figure 5-5. The Pu concentrations after short-term exposures to SGW are relatively high, ranging from 1×10^{-9} to 5×10^{-8} mol$\cdot$L^{-1}. At longer contact times, the concentrations decrease to values as low as 3×10^{-10} mol$\cdot$L^{-1} at 2000 days. However, the concentration is shown to increase to 1×10^{-9} mol$\cdot$L^{-1} after 2600 days, indicating possibly large scatter in data or perhaps a change in the mechanism leading to dissolution of precipitated Pu. In DIW, the concentration remains high, relatively independent of contact time, with a range in concentration of 1×10^{-8} to 1×10^{-7} mol$\cdot$L^{-1}. The ratio between Pu and U normalized releases is almost 10^{-2} for contact with groundwater at longer exposure times, while for DIW, the corresponding number is about 10. This is reportedly due to a combination of higher Pu concentrations and considerably lower U concentration in DIW as compared to groundwater, in which the complexation with carbonates results in an increase of several orders of magnitude in U solution concentrations.

5.1.4.2 Release of Fission Products

Long-term performance assessment models should also account for fission products with shorter half-lives, such as Cs and Sr, to cover events such as early waste package failures due to manufacturing defects or unanticipated seismic events. Under oxic conditions, Cs, Sr, Tc, and I are fairly soluble in aqueous solutions and groundwaters. However, observed variation of their release behavior indicates that the release mechanisms could be different. Cs and I have been shown experimentally to migrate to grain boundaries, fuel surfaces, and fuel cladding as a result of in-pile service (MCC, 1990). Further, at a higher linear power rating, the releases have been shown to correlate with release of the fission gases, such as Kr and Xe (MCC, 1990). Therefore, it would be expected that in short-term leaching tests, the spent fuel will release these elements at a high rate. Figure 5-6 illustrates such a rapid initial release for the ^{137}Cs under oxic conditions for the three fuel samples used in the leaching tests.

The corresponding data for ^{90}Sr shown in Figure 5-7 exhibit that, in short exposures, the ^{90}Sr release rate is fairly constant, thereafter it decreases with time similar to ^{137}Cs. Metallic inclusions of noble elements, such as Mo, Tc, Ru, Rh, and Pd, usually occur with a composition corresponding to their respective fission yields. The release of ^{99}Tc, which is usually present in abundance at or between the fuel grain boundaries in fission gas bubble sites, is believed to be controlled only by the oxidation of the inclusions. The inclusion sizes are in the nm to μm range (Thomas et al., 1989). Figure 5-8 shows ^{99}Tc release data under oxic conditions. The measured release rates for the two types of spent fuel are comparable within the wide scatter observed in the experimental data. The release rate in the range of 6×10^{-7} to 1×10^{-5}d^{-1} was maintained for a long time, leading to higher fractional release rates for ^{99}Tc than those for ^{137}Cs and ^{90}Sr after a few years (compare data in Figure 5-8 with those in Figures 5-6 and 5-7).

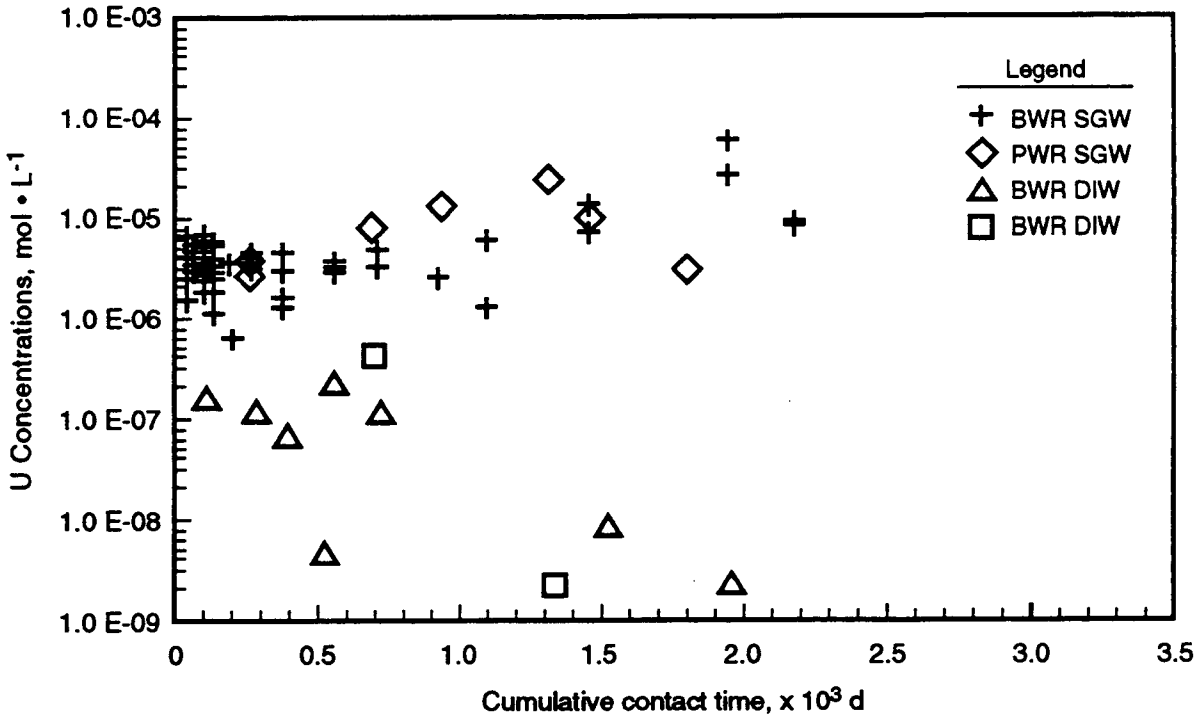

Figure 5-4. Uranium concentration in deionized water (DIW) and synthetic groundwater (SGW) as a function of cumulative contact time under oxic conditions (Forsyth and Werme, 1992)

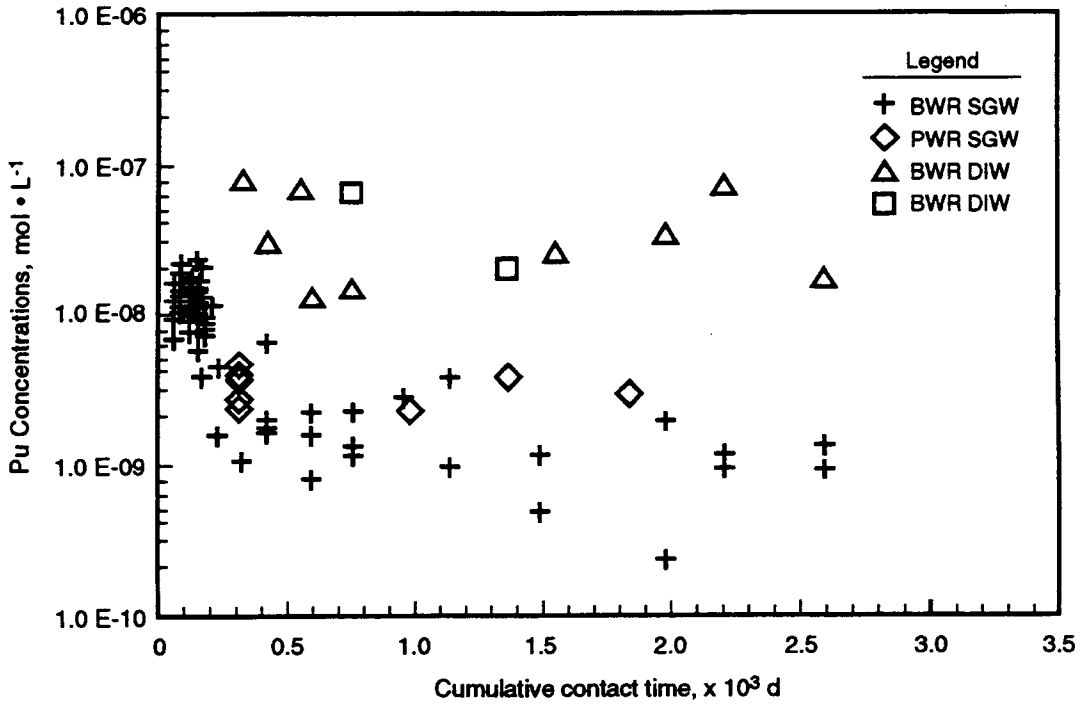

Figure 5-5. Plutonium concentrations in DIW and SGW as a function of cumulative contact time under oxic conditions (Forsyth and Werme, 1992)

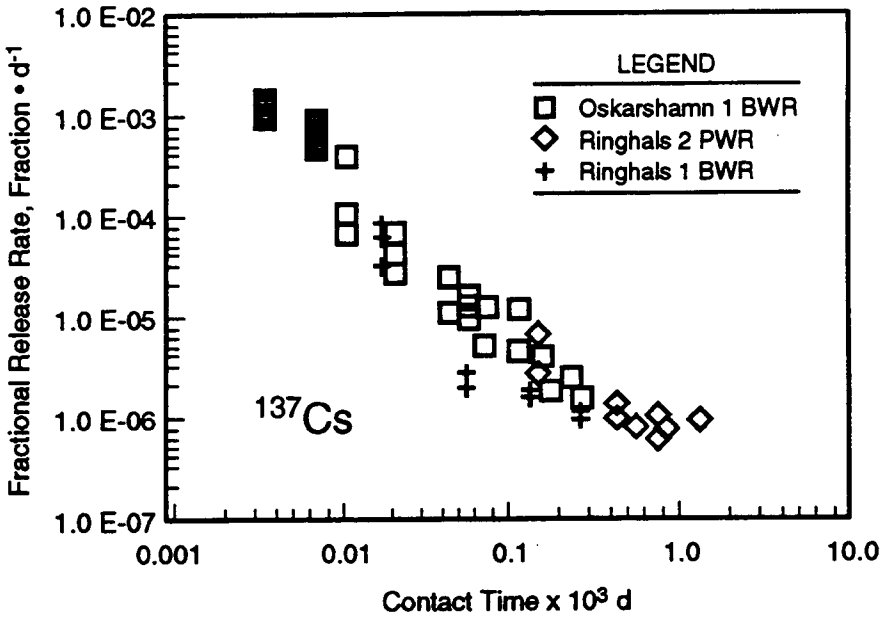

Figure 5-6. Fractional release rates for ^{137}Cs under oxic conditions (adapted from Forsyth and Werme, 1992)

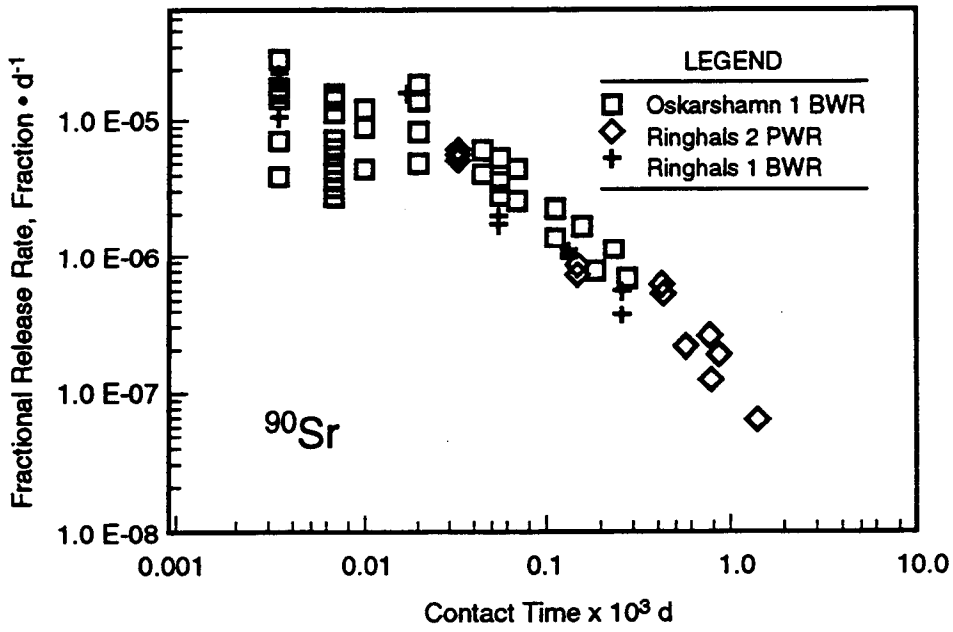

Figure 5-7. Fractional release rates for ^{90}Sr under oxic conditions (adapted from Forsyth and Werme, 1992)

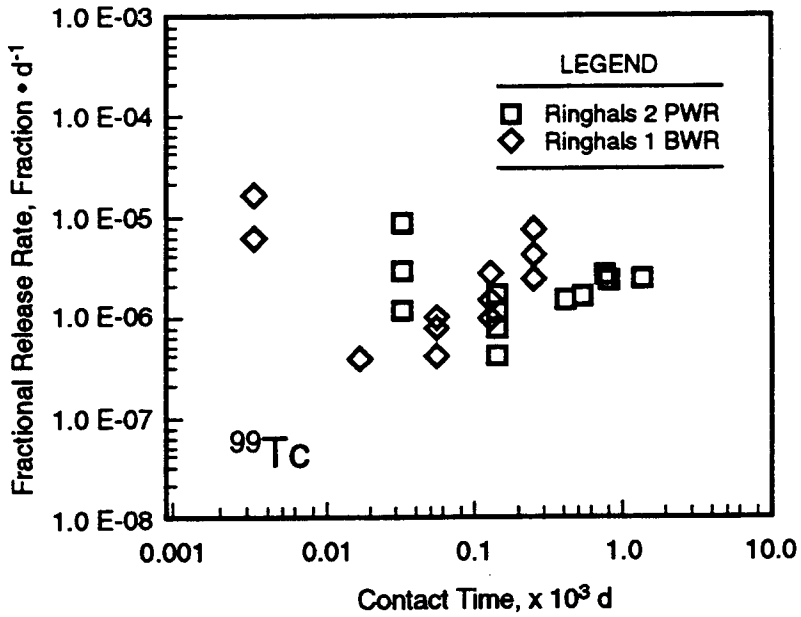

Figure 5-8. Fractional release rates for ^{99}Tc under oxic conditions (Forsyth and Werme, 1992)

5.1.5 Reducing Conditions

The effects of anoxic conditions on fractional release from a series of BWR fuel specimens are shown in Table 5-4. The change in redox condition has a major effect on the solution concentrations of ^{99}Tc, decreasing it by 2 orders of magnitude, while only minor decrease in the cumulative release fractions were noted for ^{137}Cs and ^{90}Sr. The average ^{99}Tc concentrations under reducing conditions was found to be 6×10^{-9} mol·L^{-1}. This value should be compared with a Tc solubility of 3×10^{-8} mol·L^{-1}, which is controlled by TcO_2 (a stable phase under experimental conditions). However, ^{99}Tc was also present in the fuel in metallic form (which is not readily leachable). Therefore, additional information would be required to make definitive conclusions about the release of ^{99}Tc. For ^{137}Cs and ^{90}Sr a comparison of their release rates gives more information on the mechanisms involved, as shown in Tables 5-5 and 5-6. The release of ^{137}Cs during the first 21 days of exposure is independent of redox conditions, confirming that this represents rapid initial release. During the same period, the ^{90}Sr release rate shows a more marked difference between oxic and anoxic conditions, particularly during the second contact period, where the fractional release rate decreased to $< 10^{-6}$ d^{-1} level. During the last contact period, the rates for both nuclides are below this level, even under oxic conditions, but at this stage ^{137}Cs release is more redox-dependent. For the first time, its fractional release rate under reducing conditions is lower than the rate for ^{90}Sr, suggesting an attack at sites already relatively depleted in ^{137}Cs, either during reactor operation or previous attack.

5.1.6 Comparison of Leaching Under Oxidizing Versus Reducing Environment

In a study on the radionuclide release mechanisms of spent UO_2 fuel, it is reported that U and Pu releases are much smaller for both BWR and PWR fuels under reducing conditions than those under

Table 5-4. Cumulative release fractions in a 1-y test under oxic and anoxic conditions (adapted from Forsyth and Werme, 1992)

Burnup (MWd · kgU^{-1})	Redox Condition	^{137}Cs	^{90}Sr	^{99}Tc	U	Pu
40.1	Oxic	7.8×10^{-3}	7.6×10^{-4}	1.1×10^{-3}	9.1×10^{-5}	8.7×10^{-6}
41.4	Anoxic	7.0×10^{-3}	2.1×10^{-4}	$<2.1\times10^{-3}$	$<2.1\times10^{-6}$	ND
43.8	Oxic	8.1×10^{-3}	7.5×10^{-4}	1.7×10^{-3}	9.5×10^{-5}	6.2×10^{-6}
44.9	Anoxic	7.4×10^{-3}	1.7×10^{-4}	$<2.3\times10^{-3}$	$<2.2\times10^{-6}$	ND
45.8	Oxic	8.1×10^{-3}	7.1×10^{-4}	7.3×10^{-3}	6.0×10^{-5}	8.4×10^{-6}

ND = Not Detected

Table 5-5. Rates of fractional release of ^{137}Cs under oxic and anoxic conditions (Forsyth and Werme, 1992)

Contact (days)	Oxic	Anoxic	Oxic	Anoxic	Oxic
7	1.04×10^{-3}	0.95×10^{-3}	1.01×10^{-3}	0.92×10^{-3}	0.86×10^{-3}
21	0.82×10^{-5}	1.10×10^{-5}	2.95×10^{-5}	3.45×10^{-5}	7.52×10^{-5}
63	1.56×10^{-6}	0.85×10^{-6}	1.91×10^{-6}	1.75×10^{-6}	2.39×10^{-6}
91	1.13×10^{-6}	0.23×10^{-6}	1.41×10^{-6}	0.46×10^{-6}	1.39×10^{-6}
182	8.19×10^{-7}	0.95×10^{-7}	9.82×10^{-7}	1.47×10^{-7}	9.55×10^{-7}

Table 5-6. Rates of fractional release of ^{90}Sr under oxic and anoxic conditions (Forsyth and Werme, 1992)

Contact (days)	Oxic	Anoxic	Oxic	Anoxic	Oxic
7	3.08×10^{-5}	0.32×10^{-5}	2.15×10^{-5}	0.29×10^{-5}	1.03×10^{-5}
21	1.18×10^{-5}	0.08×10^{-5}	1.42×10^{-5}	0.05×10^{-5}	1.48×10^{-5}
63	1.50×10^{-6}	1.04×10^{-6}	1.63×10^{-6}	0.26×10^{-6}	1.87×10^{-6}
91	1.00×10^{-6}	0.55×10^{-6}	1.05×10^{-6}	0.41×10^{-6}	1.12×10^{-6}
182	5.92×10^{-7}	2.81×10^{-7}	1.05×10^{-7}	0.41×10^{-7}	5.03×10^{-7}

oxidizing conditions (Werme and Forsyth, 1988). A reduction of approximately 3 orders of magnitude is exhibited by U, and of approximately 2 orders of magnitude for Pu in BWR fuel, while for PWR fuels, the trends are similar, although releases are smaller. Release of other elements such as Cs, Sr, Ba, and La are also at least an order of magnitude lower under reducing conditions than those under oxidizing conditions for BWR fuel, as shown in Figure 5-9. For PWR fuels, Sr exhibited a reduction in release of an order of magnitude under reducing conditions, while releases of Cs, Ba, and La were relatively unaffected by the change from oxidizing to reducing conditions, as shown in Figure 5-10.

5.1.7 Fuel Burnup Effects

The effect of fuel burnup is shown in Figures 5-11 and 5-12, which present the cumulative release fractions for ^{137}Cs and ^{90}Sr at various cumulative leachant contact times in oxic groundwater. Figure 5-11 shows that the release fraction for ^{137}Cs becomes practically time-independent after 28 days and varies along the fuel rod as related due to variations in burnup. The release shows an increase relative to lower burnup at a burnup of 35 $MWd \cdot kgU^{-1}$. A similar effect is exhibited by the ^{90}Sr release, but the releases continue to increase with time. For exposure times longer than 28 days, the release fractions for both nuclides attained a maximum at a burnup of about 44 $MWd \cdot kgU^{-1}$, but show an unexpected decrease at higher burnups. A similar pattern has been reported for ^{99}Tc release, while U release was quite uniform along the axial fuel length. It is possible that the increase in release fractions for Cs, Sr, and Tc observed for fuel with a burnup of about 35 $MWd \cdot kgU^{-1}$ is related to the linear power of the fuel rod, as a result of migration and concentration of these radionuclides at the grain boundaries due to axial temperature gradient within the fuel rod. However, the rapid initial release of ^{137}Cs shows a contact time dependence during the first 28 days, which is also a function of burnup. This suggests that leachant access to fuel surfaces can be at least a partial cause of the effect.

5.1.8 Flowthrough Leaching Tests

In an experimental study designed to determine the basic rate constants for the dissolution kinetics of UO_2 and spent fuel, a single-pass flowthrough method was used (Gray et al., 1992). In such a system, U concentrations remain below solubility limits allowing relatively unambiguous reaction rates to be measured. Such measurements, together with the surface areas of the test specimens, can provide relevant information for developing a kinetic model for UO_2 dissolution. The statistically designed test matrix covered four water chemistry variables: (i) temperature, 25 to 75°C, (ii) pH, 8 to 10, (iii) carbonate/bicarbonate concentration, 2×10^{-4} M to 2×10^{-2}M, and (iv) oxygen fugacity, O_2 partial pressure 0.002 to 0.2 atm. The objective was to obtain data on UO_2 and spent fuel under equivalent controlled test conditions, in the hope of conducting a majority of the future tests on unirradiated UO_2 to reduce cost. The samples were fabricated from PWR fuel with a peak burnup of 33 $MWd \cdot kgU^{-1}$ and a fission gas release of 0.25 percent.

Table 5-7 summarizes the dissolution conditions and test results. Figure 5-13 shows results typical of all ten runs. An early transient period, that usually lasted several days, was observed in each test, followed by stabilization of U dissolution rates to a nearly constant value independent of flow rate at all but the lowest flow rates. Most testing was performed at flow rates of 0.2 $ml \cdot min^{-1}$. Figure 5-14 also shows dissolution rates for ^{137}Cs, ^{99}Tc, and ^{90}Sr. An example of the flow-rate-dependent release, shown in Figure 5-14, indicates that the U concentrations were directly proportional to the reciprocal of the flow rate except at the lowest flow rates (reciprocal flow rates above 15 $min \cdot mL^{-1}$).

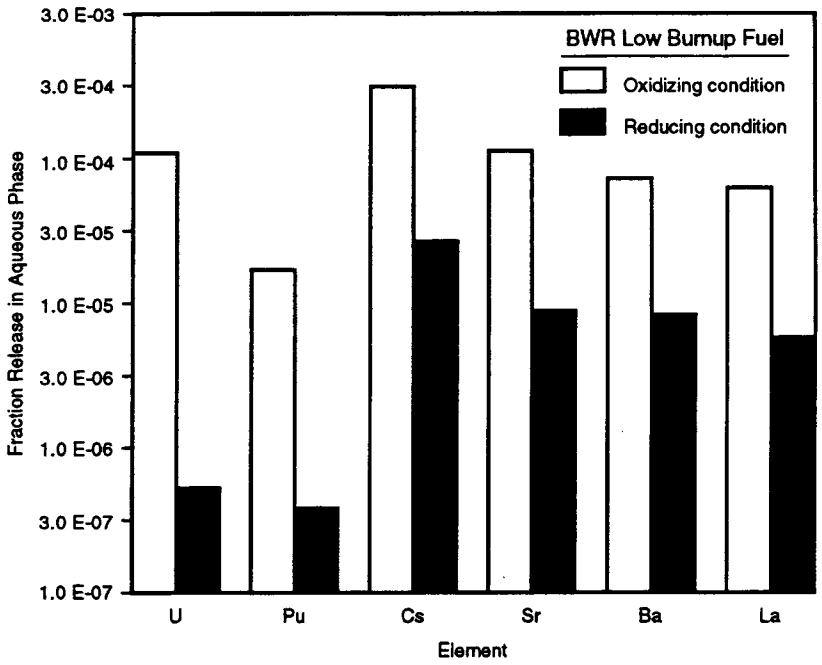

Figure 5-9. Comparison between fractional releases of uranium, plutonium, and fission products under oxidizing and reducing conditions in a low burnup BWR fuel (adapted from Werme and Forsyth, 1988)

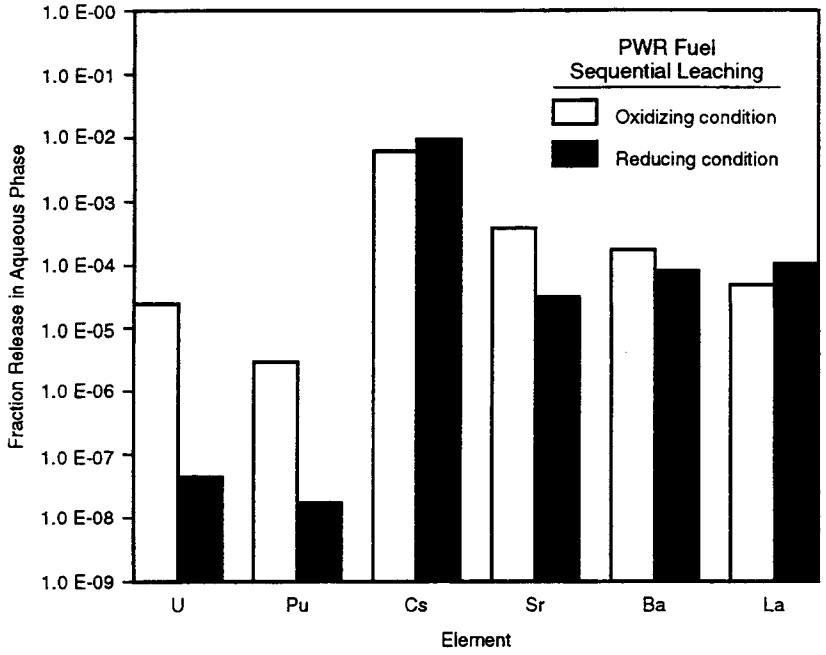

Figure 5-10. Comparison between fractional releases of uranium, plutonium, and fission products under oxidizing and reducing conditions in a PWR fuel (adapted from Werme and Forsyth, 1988)

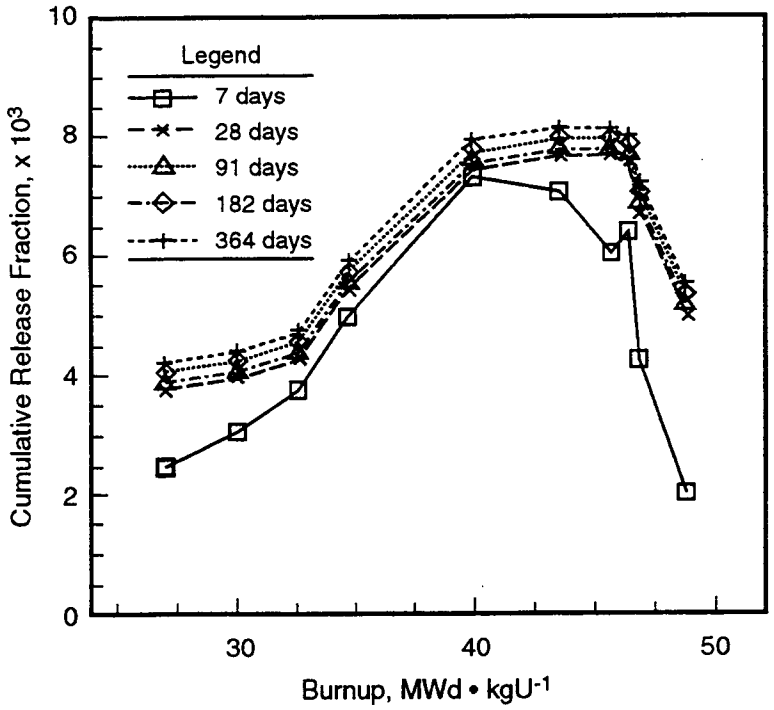

Figure 5-11. Cumulative release fractions for ^{137}Cs under oxic conditions for 7, 28, 91, 182, and 364-day leaching periods (Forsyth, 1991)

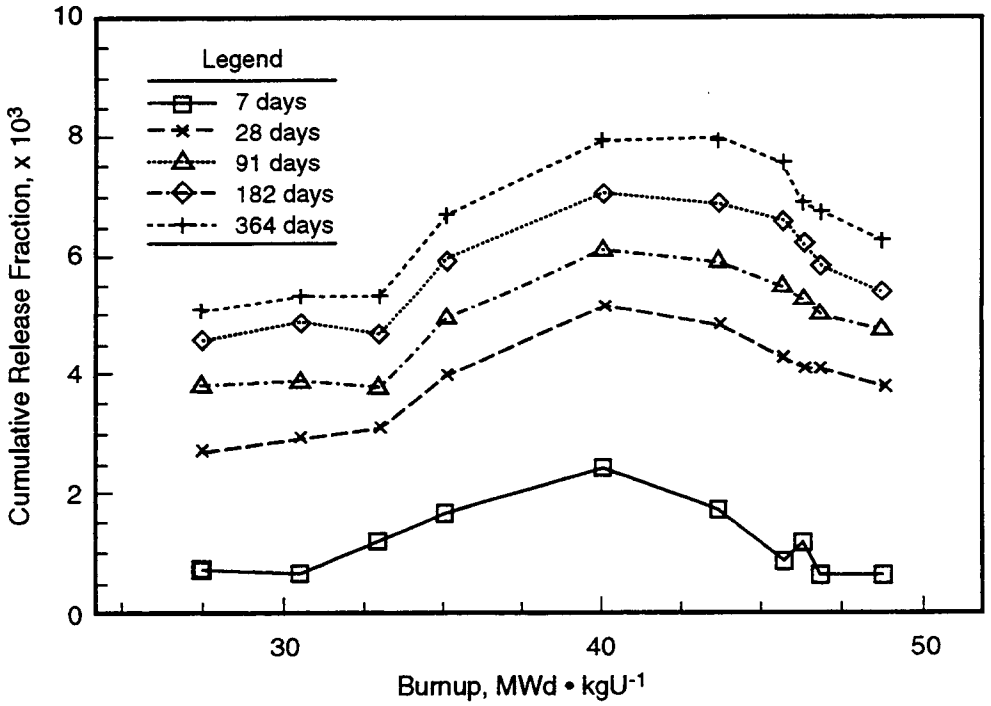

Figure 5-12. Cumulative release fractions for ^{90}Sr under oxic conditions for 7, 28, 91, 182, and 264-day leaching periods (Forsyth, 1991)

Table 5-7. Summary of spent fuel dissolution results (adapted from Gray et al., 1992)

No.	Measured Temperature (°C)	$[CO_3^{2-}] + [HCO_3^-]$ (molar) [a]	Temperature corrected pH [b]	Conc. of CO_2 (ppm) [c]	Days [d]	U dissolution rate (mg m^{-2} d^{-1})	
						Avg.	2σ [e]
1	50	2×10^{-3}	8.7 to 8.9	117	16-37	6.34	0.55
2	50	2×10^{-3}	8.7 to 8.9	117	16-37	7.05	1.44
3	50	2×10^{-3}	8.7 to 8.9	117	16-37	5.07	1.35
4	23	2×10^{-2}	8.0 to 8.2	11000	83-105, 116-130	3.45	0.51
5	75	2×10^{-2}	9.7 to 9.9	55	38-95	11.6	2.3
6 [f]	74	2×10^{-4}	7.3 to 7.9	125	22-81	8.41	1.33
6 [g]	75	2×10^{-4}	7.3 to 7.9	125	22-75	8.79	1.74
7	23	2×10^{-4}	9.7 to 10.2	0.9	37-78	0.413	0.138
8 [h]	23	2×10^{-2}	9.1 to 9.2	1030	22-59	2.83	0.30
9	23	2×10^{-3}	9.9 to 10.2	7.7	5-32	2.04	0.56

[a] Total carbonate concentration made up using appropriate amounts of Na_2CO_3 and $NaHCO_3$.

[b] pH was measured at room temperature and a calculated temperature correction was applied, where necessary.

[c] The water supply reservoirs were slowly and continuously sparged with gas containing these concentrations of CO_2, balance CO_2-free air, to stabilize the pH.

[d] Time period over which the dissolution rate was averaged. This time period eliminates the transient period as well as periods when the flow rate was low enough to yield questionable results.

[e] The standard deviation was calculated using the equation for a small number of observations. $\sigma = [\{ \Sigma(x_i - \bar{x})^2 \} / (n - 1)]^{1/2}$

[f] Same spent fuel specimen used in test 2.

[g] Fresh spent fuel specimen used.

[h] Same spent fuel specimen used in test 7.

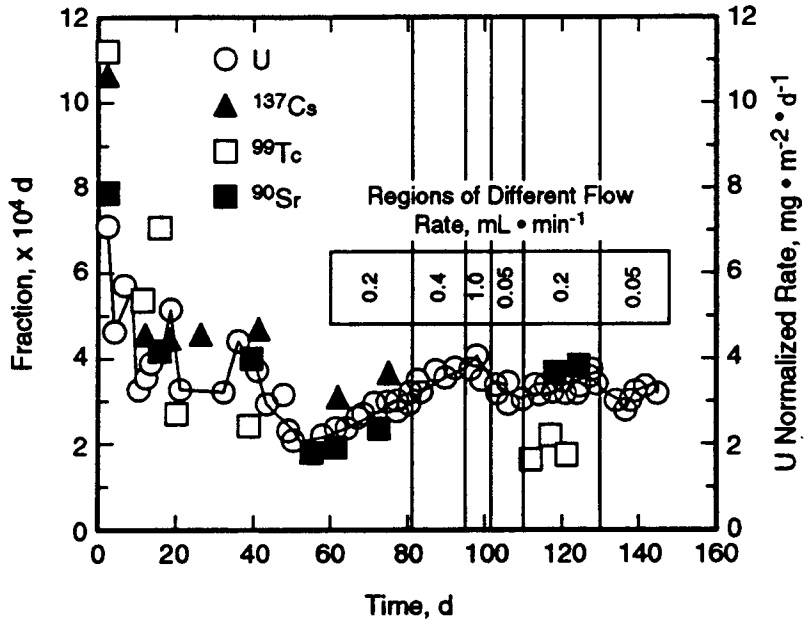

Figure 5-13. Dissolution rate of radionuclides from spent fuel grains in 2 × 10^{-2}M $NaHCO_3/Na_2CO_3$ solution at 20 to 25°C and pH 8.0 to 8.2 (Gray et al., 1992)

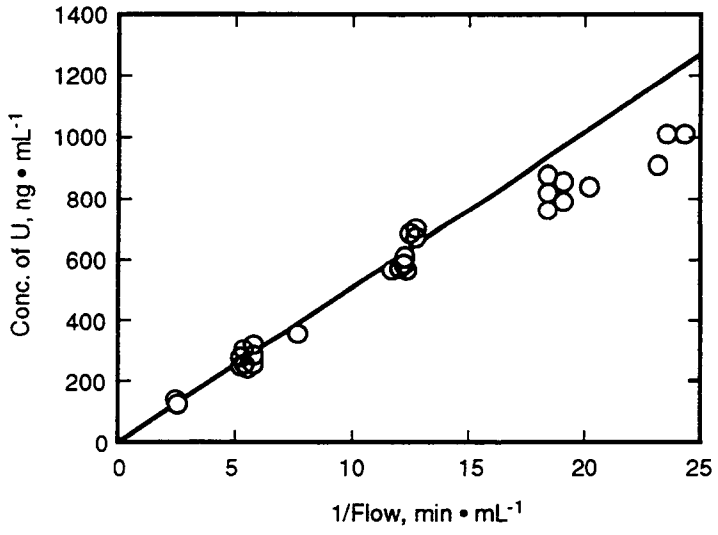

Figure 5-14. Dependence of U concentration on reciprocal flow for spent fuel grains in 2 × 10^{-2}M $NaHCO_3/Na_2CO_3$ solution at 20 to 25°C and pH 8.0 to 8.2 (Gray et al., 1992)

The analyses of the data yielded the activation energy of the dissolution process as 30 $kJ \cdot mol^{-1}$. It is reportedly higher than a value of 20 $kJ \cdot mol^{-1}$ obtained with unirradiated UO_2 in 2×10^{-3} M $NaHCO_3$ solution at pH 8.4 (Gray et al., 1992). Other literature reported estimates are 19 to 25 $kJ \cdot mol^{-1}$ between 25 and 150°C for spent fuel in groundwater containing approximately 10^{-3} M carbonate (Gray et al., 1992). Conclusions that can be drawn from the investigation, reported for 0.2 atm O_2 partial pressure only, are that the spent fuel dissolution rate exhibits a weak dependence on carbonate/bicarbonate concentration, a moderate dependence on temperature, and is nearly independent of pH over the range tested, 8 to 10.

5.1.9 Unsaturated Repository Simulating Tests

In the unsaturated repository site being investigated at Yucca Mountain, Nevada, only a limited amount of water is expected to contact the fuel under anticipated conditions. Under these circumstances, laboratory tests on spent fuel samples totally immersed in large amounts of water may only represent conditions in which flooding of the repository occurs due to water intrusions through flaws in the rock. In order to evaluate the performance of spent fuel, tests representative of other conditions for the unsaturated repository environment need to be used in spent fuel testing. In one such experimental investigation, the reaction between water and simulated wasteform under potential repository conditions was examined (Wronkiewicz et al., 1992). The method involved periodically dripping small amounts of water on samples that were maintained in temperature-regulated stainless steel test vessels. After contacting the sample, the injected water was allowed to migrate down the sides of the sample, drip from the bottom, and collect in the test vessel. The test thus simulates an environment where the waste container develops breaches along its top and bottom, allowing free flow of water through the container and limited contact time with the waste form. Sample fuel pellets were fabricated from pressed and sintered UO_2 powder with the natural isotopic abundance of U. The pellets were clad in a Zircaloy-4 tubing with bare UO_2 surfaces exposed on the top and bottom of the tubing. The leachant for the experiments was tuff-core equilibrated groundwater obtained from a well (J-13) in the vicinity of the proposed Yucca Mountain repository site. The composition of the equilibrated water (EJ-13 water) is presented in Table 5-8. Tests were conducted at a nominal temperature of 90°C.

Table 5-8. Chemical composition ($mg \cdot L^{-1}$) of EJ-13 water including carbon-containing species, anions, and cations (pH = 8.2, Solution U = 0.0024) (adapted from Wronkiewicz et al., 1992)

TOC [a]	TIC [b]	HCO_2^-	$C_2O_4^{2-}$	Cl^-	F^-	NO_2^-	NO_3^-
6.9	18.4	<0.5	<0.5	8.6	2.8	<0.5	8.2
SO_4^{2-}	B^{3+}	Li^+	Ca^{2+}	Mg^{2+}	K^+	Na^+	Si^{4+}
21	0.16	0.044	9.08	0.96	8.08	46.5	34.4

[a] = Total organic carbon
[b] = Total inorganic carbon

The results show that secondary uranyl alteration minerals began to form, and notable increases in U release occurred after the first 13 to 20 weeks of testing. This change was interpreted to reflect the onset of oxidative dissolution of the UO_2 surface and the formation of dehydrated schoepite. After approximately 1 year, samples displayed a sharp increase in U release. This rapid pulsed release is the most conspicuous feature of the entire 4.5-year reaction sequence. Sample surfaces at this stage were partially covered by dehydrated schoepite crystals, as well as minor schoepite, soddyite, and Fe-oxides. The UO_2 samples also displayed extensively corroded grain boundaries and a dusting of fine dislodged surface granules. These loosened particles were believed to be responsible for the rapid release of U noted during this interval.

After 1.5 to 2.0 years of reaction, the rapid pulsed release of U subsides, and release rates declined to an apparent steady-state level that continued up to 4.5 years. On average, only 5 mole percent of the total U released from the samples remains in solution or as suspended fine particulate matter. The remainder either settled to the bottom of the test vessel or was reprecipitated on the surfaces of test components. The top sample surfaces were found to be covered by uranyl silicate phases (uranophane, boltwoodite, and sklodowskite) that had incorporated cations from the EJ-13 water, as well as U from the dissolution of the UO_2 surfaces and/or previously deposited minerals. The similar mineralogy observed between the unsaturated tests, shown in Figure 5-15, and those of natural uraninite occurrences exposed to surfacial weathering suggests that these experiments have formed a long-term alteration sequence of uranyl silicates that may be expected to control U release in the potential repository. Both the dissolution of the UO_2 surface and the quantity of loosened fine-grained particulates on the sample surface appeared to have declined while uranyl silicates were precipitating.

The authors of the investigation conclude that although experiments conducted with UO_2 may not be entirely representative of reactions expected from spent fuel, the experiments may provide insights into the potential behavior of spent fuel dissolution since spent fuel is composed dominantly of UO_2 (Wronkiewicz et al., 1992). The experiments indicate that U release in a moist oxidizing environment will be controlled by a complex interaction of a number of processes including dissolution rates of grain boundaries, spallation of surface particles, secondary phase formation and stability, and mode of contact and composition of water with the waste form. Many of the more soluble radionuclides that migrate to the grain boundary regions during reactor operations (e.g., ^{137}Cs and ^{90}Sr) are readily mobilized during saturated dissolution tests with spent fuel (Johnson and Shoesmith, 1988). The rapid disintegration of grain boundaries, noted in the reported experiment, indicates that soluble grain nuclides segregated at grain boundaries may also be readily mobilized in an unsaturated repository environment. Furthermore, the spallation of UO_2 granules from the sample surfaces may also continuously expose new grain boundaries to corrosive fluids, thereby prolonging the release period for grain boundary radionuclides. The resultant pulsed release of U associated with spallation of UO_2 granules has implications for the release of radionuclides from the UO_2 matrix of spent fuel. Since the amount of U released in the experiments appears to be largely controlled by the migration of the fine-grained particulate matter, it follows that the migration of other radionuclides contained in the UO_2 matrix of spent fuel (Pu + Am) may be controlled by particulate dispersion rather than by solubility of the UO_2 matrix or the individual radionuclides alone. Migration of these radionuclide may now be determined by the ability of the repository hydrologic system to transport fine solids away from the waste package environment as colloidal matter. The findings of this investigation provide additional challenges to the source-term model development exercise.

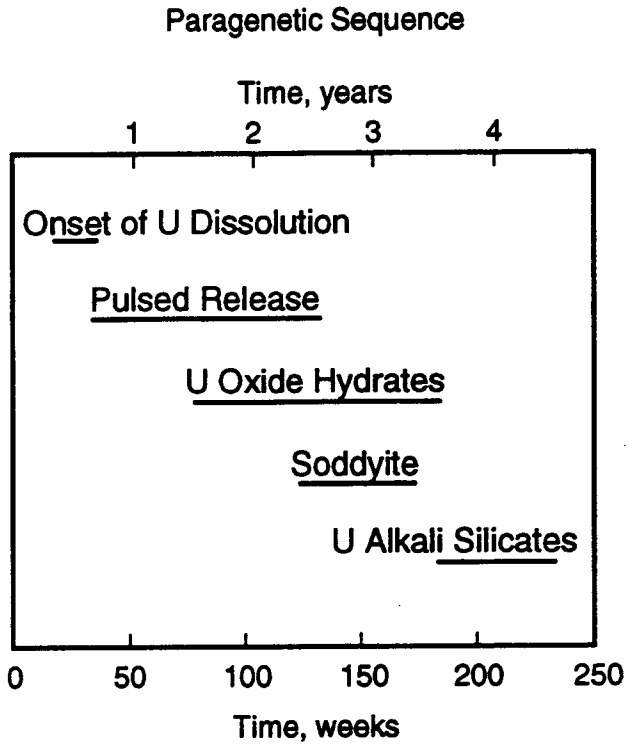

Figure 5-15. Interpretive paragenetic sequence formed on top surfaces of altered uraninite pellets. Onset of U dissolution and pulsed-release periods determined from solution data. (Wronkiewicz et al., 1992)

6 DISCUSSION OF SPENT FUEL LONG-TERM PERFORMANCE ISSUES

Source-term models are expected to provide estimates of the release of radionuclides from the waste packages under geologic repository conditions. Estimates are required for conditions that are likely to prevail for the 10,000 years of regulatory concern and for additional scenarios which could be anticipated. The reliability of the source-term model will depend on how appropriately the understanding of the quantities and characteristics of the spent fuel, waste package materials, repository environment (such as geochemistry, temperature, radiolysis products), and temporal changes in all these aspects over the 10,000 years after the repository closure are included in the model. Uncertainties in spent-fuel behavior could undoubtedly influence the evaluation (or assessment) of performance in the repository. The output of the source-term modeling exercise can be simply stated as the expression of the 'release rates and quantities' of the radionuclides from the spent fuel as a function of time over 10,000 years. The calculated releases will be compared with the allowable releases per 10 CFR 60 to judge if the repository design will provide the required level of isolation of the spent fuel. There is little uncertainty in the total inventory of the radionuclides in the spent fuel, and the task at hand would be to model release rates and cumulative releases during the 10,000-year period. A similar argument would apply to the case of vitrified (glass) wasteforms.

Based on the discussion of the inventories of the radionuclides in the cladding and spent fuel, the characteristics of the fuel and cladding (i.e., inhomogeneous distribution of the radionuclides), the oxidation behavior of the fuel, and its leaching response when in contact with moist and aqueous environments, it can be concluded that releases of radioactivity in a geologic repository will be greatly influenced by the processes considered. For an unsaturated repository, there could be extended periods of time during which the fuel may not come in contact with water, but the characteristics of the fuel may change due to oxidation in air, leading to increased surface area and release of radioactive gases in the fuel matrix. Subsequent exposure of this 'altered' spent fuel to aqueous leaching would be quite different from the event in which solid UO_2 in the pellet form comes in contact with water. The time at which the waste package fails is also critical, as it will have a bearing on the type and the amounts of radiolysis products present in the groundwaters that will contact spent fuel. Radiolysis products have a direct influence on the pH of the water, which is one of the major parameters that influence spent fuel dissolution characteristics. At the present time, only a few source-term models exist. Although a detailed review of the individual models is outside the scope of this report, a survey of the general capabilities and limitations approaches used for the development of the current source-term models indicate that some significant conclusions drawn from experimental data and analyses of the spent fuel and cladding are absent or inadequately addressed in current source-term models. Some performance factors that could modify or increase the calculated performance of the spent fuel over 10,000 years, are listed below. The literature provides a reasonable amount of data and technical information in these area, except where noted, for their inclusion in current models.

- Processes over 10,000 years of repository performance. Source-term models need to include the degradation behavior of the cladding and spent fuel during the period of exposure to high temperature (above the boiling point of water). Extended exposure at such temperatures could substantially alter the fuel characteristics, which will influence the release of radionuclides upon subsequent exposure to liquid phase groundwater. The degradation of fuel, which may be called 'alteration', will include oxidation of the fuel to higher oxidation states, substantial increase in the surface area, which will lead to increases in the calculated

release rates per unit volume of fuel, and rapid release of fission gases normally trapped in the spent UO_2 matrix.

- Use of data related to leaching behavior of spent fuel with 'altered' characteristics in modeling releases. The majority of the literature reported data are on release of radionuclides from spent UO_2 fuel rather than fuel with higher oxygen to uranium ratios, such as U_3O_8. The models should also address the scenario where a mix of unaltered spent fuel, semi-altered (quasi-equilibrium state discussed in the report), and fully altered spent fuel are releasing radionuclides in the near-field of the repository.

- Data related to leaching of spent fuel in repository specific geochemistry should be incorporated in the mechanisms which are incorporated in the models. The geochemistry should incorporate the effects of radiolysis products, leading to changes in the water pH, redox conditions, and presence of waste package corrosion products. Since the heat output of the containers with vitrified wastes is lower than containers with spent fuel, it is conceivable that these containers will corrode/breach before spent fuel containers because contact with liquid water will occur at shorter times. Under such a scenario, the geochemistry of the groundwaters will also be modified by the releases from the vitrified high-level wastes. The large number of containers with vitrified wastes (about one-third of the anticipated 40,000 to 50,000 containers) indicates that the groundwaters could contain a substantial amount of radionuclide releases from vitrified wasteforms.

- Although most source-term models acknowledge the radioactivity that might be released in the form of gases, this aspect has generally been addressed by ^{14}C releases from the crud/corrosion products on the cladding and the spent fuel. This approach will result in underestimation of the contribution of the gaseous releases from the cladding and fuel, as less than 1 percent of the wall thickness of the cladding is oxidized. An extended period of exposure of the cladding to high temperature can oxidize the cladding leading to additional release. Similarly, as stated in an earlier item, further oxidation of spent fuel in the repository will break up the fuel pellets and generate particulates leading to release of gaseous and volatile fission products to the near-field environment. Although the volume of the cladding is estimated to be less than 5 percent of the fuel, it contains approximately 50 percent of ^{14}C (the other 50 percent being in the fuel).

- Currently it is estimated that at least 1 out of every 10,000 fuel rods will be in the breached condition at the time of disposal. Although releases of radionuclides from fuel assemblies with such breached rods can be detected while in service in-reactor, individual rods are difficult to identify or remove economically. As such, it is likely that they will be disposed of along with the unbreached rods. Their distribution among the different waste packages can be known with certainty. Based on the number of containers likely to be emplaced in the first repository, one can assume 4,000 to 5,000 breached fuel rods. The radionuclide release characteristics of these rods will be different from the unbreached rods under most repository scenarios. The contribution of the breached rods to the source term will be considerable, and needs to be accounted for. Current models assume no breached rods.

- According to the SCP design, it is estimated that there will be approximately 1,000 fuel rods per waste package. The DOE in assuming 'no-credit' for the cladding assumes that upon failure of a given waste package, fuel contained in all 1,000 rods will be exposed to the

repository environment. This may neither be a realistic situation nor even a conservative one. For instance, if the failure of the waste package is due to flooding of the repository leading to corrosion of the metallic container, we are assuming that spent UO_2 fuel contained in approximately 1,000 rods inside the waste package is exposed simultaneously to groundwater. Under such a scenario, the source-term model will use leaching mechanisms and experimental data related to leaching of 'unaltered' spent fuel to calculate release of radionuclides. This scenario is inconsistent with a distribution of failure of the cladding with time, which would lead to alteration of the spent fuel, e.g., substantially increased surface area per unit volume, different release mechanism, rapid release of fission gases, etc. Therefore, the source-term models need to incorporate a distribution of cladding failure as a function of time.

- Most current source-term models are based on the assumption that maximum release of a particular radionuclide in the leachant (groundwater) will be limited (controlled) by the solubility limit of that radionuclide. This assumption would be valid provided 100 percent of the release of all radionuclides were in solution in the aqueous phase. There is evidence that such is not always the case. A number of elements are likely to occur in the form of colloids and precipitates in a geologic repository. Since the precipitates and colloids are not in solution, they provide an add-on term to the source-term models. Although, the fraction of releases of actinides known to form of colloids and precipitates in not known precisely at present, the assumption used in some elementary treatments in source-term models of a maximum of 30 percent could be a gross underestimation.

- The presence of organic material and microbes in water is known to influence the migration of radionuclides in underground environments. Microbial activities expected in an unsaturated repository may provide a significant add-on term to the source-term modeling and needs to be investigated. Since the studies related to microbial activities and their influence on the alteration of spent-fuel characteristics are practically non-existent, additional experimental investigations in this area are warranted to estimate the contribution of the potential microbial activities to the source-term.

- The EBS components are expected to be constructed from a number of materials. Most studies related to the failure of the waste package concentrated on the corrosion failure of the metallic container as a result of groundwater/container interaction, and do not address electrochemical effects between the fuel and the cladding and the fuel and the container material. Insufficient consideration of potential galvanic effects in selecting waste package materials could adversely affect the fuel cladding failure distribution as a function of time and could also accelerate the spent fuel degradation/dissolution. Therefore, electrochemical interactions between the waste package materials, spent fuel cladding, and the spent fuel need to be evaluated and possibly incorporated in the source-term models.

7 REFERENCES

Adachi, T., T. Muromura, H. Takeishi, and T. Yamamoto. 1988. Metallic phases precipitated in UO_2 fuel: II. Insoluble residue in simulated fuel. *Journal of Nuclear Materials* 160: 81-87.

Andrews, M.G., H.R. Freeburn, and W.D. Wohlsen. 1979. Performance of combustion engineering fuel in operating PWRs. *American Nuclear Society Topical Meeting—LWR Fuel Performance*. La Grange Park, IL: American Nuclear Society (ANS). 11-19.

Bailey, W.J., A.B. Johnson, Jr, and R.W. Lambert. 1986. Integrity of spent fuel and pool components during wet storage. *Transactions of the American Nuclear Society*. 50: 116.

Bailey, W.J., and A.B. Johnson, Jr. 1990. The expected condition of spent fuel on delivery to a repository. *High Level Radioactive Waste Management*. La Grange Park, IL: ANS. 1437-1443.

Bailey, W.J., and M. Tokar. 1982. *Fuel Performance Annual Report for 1981*. Washington, DC: U.S. Nuclear Regulatory Commission (NRC).

Baily, W.E., J.S. Armijo, J. Jacobson, and R.A. Proebstle. 1979. BWR fuel performance. *American Nuclear Society Topical Meeting—LWR Fuel Performance*. La Grange Park, IL: ANS. 1-10.

Barner, J.O. 1984. *Characterization of LWR Spent Fuel MCC-Approved Testing Material—ATM-101*. PNL-5109. Richland, WA: Pacific Northwest Laboratories (PNL).

Bell, M.J. 1973. ORIGEN. *The ORNL isotope generation and depletion code*. ORNL-428. Oak Ridge, TN: Oak Ridge National Laboratory (ORNL).

Bennett, M.J., J.B. Price, and P. Wood. 1987. Influence of manufacturing route and burnup on the oxidation and fission gas release behavior of irradiated uranium dioxide in air at 175-400°C. *Proceedings of the International Workshop on Chemical Reactivity of Oxide Fuel and Fission Product Release*. Harwell, UK: United Kingdom Atomic Energy Agency (UKAEA).

Bowman, S.M. 1992. PC input processor for ORIGEN-S. *Proceedings of the Third International Conference on High Level Radioactive Waste Management*. La Grange Park, IL: ANS. 88-92.

Bradley, R.E., W.J. Bailey, A.B. Johnson, Jr., and L.M. Lowry. 1981. *Examination of zircaloy-clad spent fuel after extended pool storage*. PNL-3921. Richland, WA: PNL.

Brodda, B.G., and E.R. Merz. 1984. The leaching behavior of zircaloy cladding and its impact on the conditioning of waste for final disposal. *Nuclear Technology*. 65: 432-437.

Croff, A.G. 1983. ORIGEN-2: A versatile computer code for calculating the nuclide compositions and characteristics of nuclear materials. *Nuclear Technology*. 62: 335-352.

Cubicciotti, D., J.S. Sanecki, R.W. Strain, S. Greenberg, L.A. Neimark, and C.E. Johnson. 1976. *The nature of fission product deposits inside LWR Fuel Rods*. SRI Project No. 4197. Menlo Park, CA: SRI International.

Einziger, R.E., S.C. Marschman, and H.C. Buchanan. 1991. Spent-Fuel Dry-Bath oxidation testing. *Nuclear Technology*. 94: 383-393.

Einziger, R.E., S.D. Atkin, D.E. Stellrecht, and V. Pasupathi. 1982. High temperature postirradiation materials performance of spent PWR fuel rods under dry storage conditions. *Nuclear Technology*. 57: 65-80.

Einziger, R.E. 1991. Effects of an oxidizing atmosphere in a spent fuel packaging facility. *FOCUS'91—Conference on Nuclear Waste Packaging*. La Grange, Park, IL: ANS.

Einziger, R.E., and R.V. Strain. 1986. Behavior of breached PWR spent-fuel rods in an air atmosphere between 250°C and 360°C. *Nuclear Technology*. 75: 82-95.

EPRI. 1989. *Fuel consolidation demonstration: Spent fuel storage area analysis*. EPRI NP-6551. Palo Alto, CA: Electric Power Research Institute (EPRI).

EPRI. 1984. *Surveillance of LWR spent fuel in wet storage*. EPRI-NP-3765. Palo Alto, CA: EPRI.

EPRI. 1986. *Fuel and pool component performance in storage pools*. EPRI-NP-4651. Palo Alto, CA: EPRI.

Fish, R.L., and R.E. Einziger. 1981. *A perspective on fission gas release from spent fuel rods during geologic disposal*. HEDL-TME 81-3. Richland, WA: Hanford Engineering Development Laboratory (HEDL).

Forsyth, R.S. 1991. Spent fuel degradation. Scientific Basis of Nuclear Waste Management XIV. Pittsburgh, PA: Materials Research Society (MRS). 212: 177-188.

Forsyth, R.S., and L.O. Werme. 1992. Spent fuel corrosion and dissolution. *Journal of Nuclear Materials* 190: 3-19.

Garzarolli, F., R. von Jan, and H. Stehle. 1979. Main causes of fuel element failure in water-cooled power reactors. *Atomic Energy Review*. 17: 31-128.

Gilbert, E.R., W.J. Bailey, A.B. Johnson, Jr., and M.A. McKinnon. 1990. Advances in technology for storing LWR spent fuel. *Nuclear Technology*. 89: 141-161.

Gray, W.J., H.R. Leider, and S.A. Steward. 1992. Parametric study of LWR spent fuel dissolution kinetics. *Journal of Nuclear Materials* 190: 46-52.

Guenther, R.J. 1983. *Results of simulated abnormal heating events for full-length nuclear fuel rods*. PNL-4555. Richland, WA: PNL.

Guenther, R.J., D.E. Blahnik, T.K. Campbell, U.P. Jenquin, J.E. Mendel, L.E. Thomas, and C.K. Thornhill. 1988. *Characterization of spent fuel approved testing material ATM 103*. PNL-5109-103. Richland, WA: PNL.

Guenther, R.J., D.E. Blahnik, T.K. Campbell, U.P. Jenquin, J.E. Mendel, L.E. Thomas, and C.K. Thornhill. 1991. *Characterization of spent fuel approved testing material ATM 105.* PNL-5109-105. Richland, WA: PNL.

Guenther, R.J., and J.O. Barner. 1981. *Performance of Annular-Coated, Annular, Vipac, and Reference Test Rods During Steady-State Irradiation in HBWR IFA-518.1.* PNL-3952 (DOE/ET/34215-23): Richland, WA: PNL.

Guenther, R.J., E.R. Gilbert, S.C. Slate, W.L. Partain, J.R. Divine, and D.K. Kreid. 1984. *Assessment of degradation concerns for spent fuel, high level wastes, and transuranic wastes in monitored retrievable storage.* PNL-4879. Richland, WA: PNL.

Guenther, R.J., D.E. Blahnik, L.E. Thomas, D.L. Baldwin, and J.E. Mendel. 1990. Radionuclide distribution in LWR spent fuel. *Proceedings of SPECTRUM'90 - Nuclear and Hazardous Waste Management International Topical Meeting.* La Grange Park, IL: ANS. 120-123.

Heeb, C.M., M.A. McKinnon, and J.M. Creer. 1990. ORIGEN-2 predictions of spent fuel decay heat rates and isotopic content compared with calorimeter and key actinide measurements. *Proceedings of SPECTRUM'90—Nuclear and Hazardous Waste Management International Topical Meeting.* La Grange Park, IL: ANS. 116-119.

Hirabayashi, T., T. Sato, C. Sagawa, N.M. Masaki, M. Saeki, and T. Adachi. 1990. Distributions of radionuclides on and in spent nuclear fuel claddings of PWRs. *Journal of Nuclear Materials* 174: 45-52.

Johnson, A.B., Jr. 1977. Behavior of spent nuclear fuel in water pool storage. BNWL-2256. Richland, WA: Battelle Pacific Northwest Laboratories (BPNL).

Johnson, A.B., Jr. 1979. Spent fuel storage experience. *Nuclear Technology.* 43: 165-173.

Johnson, A.B., Jr., E.R. Gilbert, and R.J. Guenther. 1982. *Behavior of spent nuclear fuel and storage system components in dry interim storage.* PNL-4189. Richland, WA: PNL.

Johnson, A.B., Jr., and E.R. Gilbert. 1983. *Technical basis for storage of zircaloy-clad fuel in inert gases.* PNL-4835. Richland, WA: PNL.

Johnson, E.R. 1986. Centralized disassembly and packaging of spent fuel in the DOE spent fuel management system. *Transactions of the American Nuclear Society.* 52: 73-74.

Johnson, L.H., and D.W. Shoesmith. 1988. Spent fuel. *Spent Fuel, Radioactive Waste Forms for the Future.* W. Lutze and R.C. Ewing, ed. North-Holland Physics Publishing, Amsterdam, The Netherlands. 635-698.

Johnson, L.H., D.W. Shoesmith, G.E. Lunansky, M.G. Bailey, and P.R. Tremaine. 1982. The mechanisms of leaching and dissolution for UO_2 fuel pellets under simulated disposal conditions: *Nuclear Technology.* 56: 238-253.

Katayama, Y.B., D.J. Bradley, and C.O. Harvey. 1980. *Status report on LWR spent fuel IAEA leach tests*. PNL-3173. Richland, WA: PNL.

Klein, J.A. 1987. The integrated database program: An executive database of spent fuel and radioactive waste inventories, and characteristics. *Proceedings of the WASTE MANAGEMENT '87 Symposium*. Tucson, AZ: University of Arizona. 483-488.

Kleykamp, H. 1979. The chemical state of LWR high-power rods under irradiation. *Journal of Nuclear Materials* 84: 109-117.

Locke, D.H. 1975. Review of experience with water reactor fuels — 1968-1973. *Nuclear Engineering and Design*. 33: 94-124.

Manaktala, H.K. 1990. Potential degradation modes of spent fuel zirconium alloy cladding in a geological repository environment. *Ninth International Symposium on Zirconium in the Nuclear Industry*. Kobe, Japan. American Society for Testing and Materials (ASTM).

Manaktala, H.K. 1991. Degradation Modes of Nuclear Reactor Fuel Cladding. Paper No. 91037. *CORROSION/91*. Houston, TX: National Association of Corrosion Engineers (NACE).

Moore, R.S., K.J. Notz, and C.G. Lawson. 1990. Classification of LWR defective fuel data. *Proceedings of the SPECTRUM'90 Nuclear and Hazardous Waste Management International Topical Meeting*. La Grange Park, IL: ANS. 129-132.

Moore R.S., and K.J. Notz,. 1991. Tools for LWR spent fuel characterization: Assembly classes and fuel designs. *Proceedings of the Second Annual International Conference on High Level Radioactive Waste Management*. La Grange Park, IL: ANS. 1: 91-95.

Notz, K.J., R. Salamon, T.D. Welch, R.J. Reich, and R.S. Moore. 1992. Spent fuel characteristics provided by the CDB — An Update. *Proceedings of the Third International Conference on High Level Radioactive Waste Management*. La Grange Park, IL: ANS. 122-130.

Ocken, H. 1982. Fission gas release from fuel rods irradiated in U.S. commercial LWR. *American Nuclear Society Topical Meeting on LWR Extended Burnup—Fuel Performance and Utilization*. La Grange Park, IL: ANS. 3/59-3/75.

Olander, D.R. 1976. *Fundamental aspects of nuclear reactor fuel elements*. TID-26711-P1. Technical Information Center. Energy Research and Development Administration. Oak Ridge, TN: ORNL.

Parks, C.V. 1992. Overview of ORIGEN-2 and ORIGEN-S: Capabilities and Limitations. *Proceedings of the Third International Conference on High Level Radioactive Waste Management*. La Grange Park, IL: ANS. 57-64.

Pearcy, E.C., and H. K. Manaktala. 1992. Occurrence of metallic phases in spent nuclear fuel: Significance for source term predictions for high level waste disposal. *Proceedings of the Third*

International Conference on High Level Radioactive Waste Management. La Grange Park, IL: ANS. 131-136.

PNL. 1990. Materials Characterization Center (MCC) Burnup and Fission Gas Release Distribution Workshop. Seattle, WA. June 27-28, 1990. Richland, WA: PNL.

Thomas, L.E., R.E. Einziger, and R.E. Woodley. 1989. Microstructural Examination of Oxidized Spent PWR Fuel by Transmission Electron Microscopy. *Journal of Nuclear Materials* 166: 243-251.

Tsoulfanidis, N., and R.G. Cochran. 1991. Radioactive waste management. *Nuclear Technology*. 93: 263-304.

U.S. DOE. 1992a. *Characteristics of Potential Repository Wastes*. DOE/RW-0184-R1. Washington, DC: U.S. Department of Energy (DOE).

U.S. DOE. 1992b. *Spent Nuclear Fuel Discharged from U.S. Reactors 1990*. SR/CNEAF/92-01.

U.S. DOE. 1982. *Spent Fuel and Radioactive Waste Inventories, Projections, and Characteristics*. DOE/NE-0017-1.

U.S. DOE. 1988a. *Characteristics of Spent Fuel, High-Level Waste, and Other Radioactive Wastes Which May Require Long-Term Isolation*. DOE/RW-0184. Oak Ridge, TN: ORNL. Vol. 1-6.

U.S. DOE. 1988b. *Characteristics of Spent Fuel, High-Level Waste, and Other Radioactive Wastes Which May Require Long-Term Isolation*. DOE/RW-0184. Oak Ridge, TN: ORNL. Vol. 7-8.

U.S. NRC. 1990. Title 10 U.S. Code of Federal Regulations Part 60. Disposal of High-Level Radioactive Wastes in Geological Repositories. *Office of the Federal Register*: Washington, DC: NRC.

VanLuik, A.E., M.J. Apted, W.J. Bailey, J.H. Haberman, J.S. Shade, R.E. Guenther, R.J. Serne, E.R. Gilbert, R. Peters, and R.E. Williford. 1987. *Spent fuel as a waste form for a geologic disposal: Assessment and recommendation on data and modeling needs*. PNL-6329. Richland, WA: PNL.

Welch, T.D., K.J. Notz, and R.J. Andermann, Jr. 1990. Important parameters in ORIGEN2 calculations of spent fuel compositions. *Proceedings of SPECTRUM'90 Nuclear and Hazardous Waste Management International Topical Meeting*. La Grange Park, IL: ANS. 133-136.

Welch, T.D., and K.J. Notz, 1990. Utilization of ORIGEN-2 by the characteristics database. *Proceedings of SPECTRUM'90—Nuclear and Hazardous Waste Management International Topical Meeting*: La Grange Park, IL: ANS. 72-76.

Werme, L.O., and R.S. Forsyth. 1988. Spent UO_2 fuel corrosion in water: Release mechanisms. Scientific Basis of Nuclear Waste Management XI. Philadelphia, PA: MRS. 112: 443-452.

Williamson, R., and S.A. Beetham. 1987. Fission product and U_3O_8 particulate emission arising from the oxidation of irradiated UO_2: Preliminary studies. *Proceedings of the International Workshop on Chemical Reactivity of Oxide Fuel and Fission Product Release*. Berkeley, U.K.

Wood, P., M.J. Bennett, M.R. Houlton, and J.B. Price. 1985. Oxidation and fission gas release behavior of irradiated uranium dioxide in air below 400°C. *Proceedings of the BNES Conference on Nuclear Fuel Performance*. Stratford-on-Avon, U.K.

Woodley, R.E. 1983. *The characteristics of spent LWR fuel relevant to its storage in geologic Repositories*. HEDL-TME 83-28. Richland, WA: HEDL.

Woodley, R.E., R.E. Einziger, and H.C. Buchanan. 1989. Measurement of the oxidation of spent fuel between 140°C and 225°C. *Nuclear Technology*. 85: 74-88.

Wronkiewicz, D.J., J.K. Bates, T.J. Gerding, E. Veleckis, and B.S. Tani. 1992. Uranium release and secondary phase formation during unsaturated testing of UO_2 at 90°C. *Journal of Nuclear Materials* 190: 107-127.

Wuertz, R., and M. Ellinger. 1985. Source term for the actinide release from a repository for spent LWR fuel. Scientific Basis of Nuclear Waste Management IX. Philadelphia, PA: MRS. 50: 393-400.

Yang, R.L., and D.R. Olander. 1981. Behavior of metallic inclusions in uranium dioxide. *Nuclear Technology*. 54: 223-233.

Zacha, N.J. 1988. Fuel rod consolidation. *Nuclear News*. 31:(3) 68-73.

Zima, G.E., 1979. *An Evaluation of Potential Chemical/Mechanical Degradation Processes Affecting Fuel and Structural Materials under Long-Term Water Storage*. NUREG/CR-0668. Washington, DC: NRC.